IEEE Access
Multidisciplinary | Rapid Review | Open Access Journal

Received 24 October 2023, accepted 16 December 2023, date of publication 4 January 2024,
date of current version 12 January 2024.

Digital Object Identifier 10.1109/ACCESS.2024.3349594

RESEARCH ARTICLE

Optimal Design and Performance Analysis of Hybrid Renewable Energy System for Ensuring Uninterrupted Power Supply During Load Shedding

MUHAMMAD PAEND BAKHT[1,2], MOHD NORZALI HAJI MOHD[1], (Senior Member, IEEE), USMAN ULLAH SHEIKH[3], AND NUZHAT KHAN[4]

[1]Faculty of Electrical and Electronics Engineering (FKEE), Universiti Tun Hussain Onn Malaysia, Parit Raja 86400, Malaysia
[2]Department of Electrical Engineering, Balochistan University of Information Technology, Engineering and Management Sciences, Quetta 87300, Pakistan
[3]Faculty of Electrical Engineering, Universiti Teknologi Malaysia, Johor Bahru 81310, Malaysia
[4]School of Industrial Technology, Universiti Sains Malaysia, Gelugor 11800, Malaysia

Corresponding authors: Mohd Norzali Haji Mohd (norzali@uthm.edu.my), Usman Ullah Sheikh (usman@fke.utm.my), and Nuzhat Khan (Nuzhat_khan@usm.edu.my)

This work was supported in part by Universiti Tun Hussein Onn Malaysia (UTHM) and the UTHM Publisher's Office through Publication Fund under Grant E15216, and in part by the Ministry of Education Malaysia and Universiti Teknologi Malaysia (UTM) through the UTM Fundamental Research Grant under Grant Q.J130000.3823.22H29.

ABSTRACT Given the significant impact of the UN 2015 agenda on sustainable development, the search for eco-friendly and efficient energy solutions has intensified. The renewable based hybrid systems have emerged as feasible solution in this context. This paper explores the potential of utilizing a hybrid energy system (HES) from a distinctive perspective — addressing the challenges of load shedding at the distribution level. The HES configuration in this investigation includes photovoltaic (PV) array, wind turbines (WT), battery storage unit (BSU) and diesel generator system. The research involves simulations, optimization, and sensitivity analysis for a residential community in the southwestern part of Pakistan, which frequently experiences load shedding. Grasshopper optimization algorithm (GOA) is applied to simultaneously minimize the levelized electricity cost (LEC), payback period (PBP), and loss of power supply probability (LPSP). Simulations compare different HES configurations based on the estimation of local renewable energy potential and the load shedding schedule of the utility company. The optimal solution, with N_{PV} =110, N_{WT} =2, and N_{BSU} =16, was selected, resulting in a minimum LEC of 6.64 cents/kWh and a PBP of 7.4 years. These results are validated using the particle swarm optimization algorithm (PSO). The performance of HES is benchmarked against conventional solutions, such as standalone diesel generators, battery-based uninterruptible power supplies (UPS), and combinations of generators and UPS. The findings demonstrate the significant superiority of HES over conventional solutions in terms of reduced LEC, shorter PBP and reduced carbon emissions. Finally, the sensitivity analysis examines the impact of varying component prices, feed-in tariff rates, meteorological conditions, and load demand variations on the LEC and PBP of the HES.

INDEX TERMS Optimization, renewable, photovoltaic, wind turbine, power outage, multi criteria, feed in tariff, payback period, breakeven.

I. INTRODUCTION

The uninterrupted power supply or in other words the continuous provision of electricity supply to consumers, is considered as the basic need of the modern world. However,

The associate editor coordinating the review of this manuscript and approving it for publication was Bijoy Chand Chatterjee.

for many developing nations, the energy shortfall remains an issue due to various factors including insufficient generation capacity, inefficiencies in power transmission and inadequate or outdated distribution infrastructure [1]. In addition, rapid population growth and the lack of investment in power infrastructure (including national grid) add to further stress on the system. As a result, grid operators are forced to resort to load shedding to sustain the system at its current level. Load shedding is a power system control procedure intended to reduce or limit a specific amount of electrical load when the demand for electricity surpasses the supply capacity of the network [2]. The operator deliberately turns off the supply to some parts of electrical network, with the objective of maintaining a balance between generation and supply [3]. Typically, the load is cut-off (with an informed time-schedule) in different parts of distribution network for non-overlapping phases of time. Although the shedding results in loss of supply for certain parts of the grid network, it ensures system stability and avoids the systemic supply collapse.

Integrating renewable energy sources (RES) into the grid can offer a promising solution for the load shedding problem. This solution is particularly advantageous for regions blessed with abundant RES such as wind, solar, and tidal/ocean wave. However, it is essential to acknowledge that RES like solar and wind possess inherent intermittency, which can present challenges in maintaining a consistent power supply. To handle this situation, it is recommended to augment renewable energy installations with a robust energy storage system, such as battery storage. Battery system can store excess energy generated during periods of high renewable energy production and discharge it when demand exceeds supply, effectively mitigating the impact of intermittency. The combination of RES with batteries and/or diesel generator is popularly known as the hybrid energy system (HES). The HES can operate in a grid connected or off grid (standalone) mode. These systems have been increasingly recognized for their significant technical, economic, and environmental advantages [4], [5]. Some of their direct benefits include energy bill reductions, improved energy security, enhanced resiliency, and reduced emissions. For the load shedding scenario, the unique capability of HES to seamlessly operate in off-grid mode can provide invaluable support. Despite these advantages, the incorporation of multiple energy sources necessitates careful considerations throughout the planning and analysis phases. Some critical aspects include selecting appropriate technologies, determining the optimal size of the sources, simulating the efficient operation to meet reliability criteria and constraints, assessing the financial feasibility of the system, and effectively managing risks associated with intermittencies.

The existing literature on HES can be broadly categorized into two main types: off-grid systems and grid-connected systems. These two categories exhibit fundamental differences, particularly in the context of load shedding. Off-grid systems, being stand-alone and not connected to the main electrical grid, are typically not affected by load shedding concerns. On the other hand, grid-connected HES predominantly rely on RES but resort to the grid in case of RES power falls short to meet the load demand, often aiming at objectives like cost and emissions reduction etc. However, when considering the unique scenario of load shedding, the applicability of existing studies becomes limited. This is due to the fact that load shedding introduces system vulnerability as the grid cannot meet the entire load demand. This situation will potentially result in system instability or power disruptions when RES power is unavailable. For HES, the situation becomes even more complicated as supply cut-offs must synchronize with the intermittency of RES and varying loads. Inevitably, the optimization becomes imperative to achieve efficient operation of HES. The optimization must concurrently address multiple constraints, including renewable intermittency, varying demand, battery storage state of charge, and the generator fuel consumption (if utilized). Many studies have been conducted on HES optimization encompassing aspects such as system sizing, planning, energy management, and control. These investigations have employed either deterministic methods [6], [7] or metaheuristic techniques. References [8] and [9] to achieve optimization objectives. Considering diverse variable types, non-linearity, and non-convex nature of the system, deterministic methods are less effective and often encounter convergence issues. Consequently, metaheuristic algorithms emerge as more effective methods for optimizing HES [10]. Some commonly employed algorithms are particle swarm optimization (PSO), cuckoo search (CS), genetic algorithm (GA), simulated annealing (SA), bee algorithm (BA) and grasshopper optimization (GOA). In light of the foregoing, this research utilizes GOA and PSO to design and optimize HES for the load shedding problem effectively. GOA, a relatively recent algorithm, has demonstrated successful applications in various sizing problems, for example [11] and [12]. Conversely, PSO, an established algorithm with a substantial track record, has found extensive use across a wide range of applications [13]. Compared to the existing studies, significant contributions and novelties of this work are:

A. Providing the in-depth analysis of different load shedding mitigation methods which include demand side management (DSM) strategies, conventional and modern methods such as hybrid system.
B. Assessing the feasibility of HES with a actual case study of residential community undergoing daily load shedding situated in Quetta city, a south western part of Pakistan. The considered HES technologies include photovoltaic modules (PV), wind turbines (WT), battery storage unit (BSU) and diesel generator (Gen) system.
C. Investigating the most feasible techno-economic HES for load shedding problem through optimization framework.
D. Performing a comprehensive techno-economic and environmental comparison of HES with conventional

solutions including diesel generator battery-based UPS system.

E. Conducting a sensitivity analysis to observe HES response against variations in certain input parameters of load demand, cost and weather conditions.

II. RESEARCH BACKGROUND

Power system is primarily designed to maintain a balance between generation and consumption. Traditionally, the generation is realized by the centralized power stations, while the consumption is manifested in the form of load demand [14]. When there's a mismatch between generation capacity and demand, supply availability and system stability are compromised. In AC systems operating at 50/60 Hz, such imbalances cause frequency fluctuations, risking synchronization loss and system instability [15]. To address this, power system designers employ protection and control strategies, including automatic generation control and load control (see Table 1). These proactive measures are essential to prevent the loss of generation capacity, equipment damage, and blackouts [16].

TABLE 1. Power system frequency relationship with generation and load.

Condition	Frequency	Effect
Generation > Demand + Losses	Increase	Automatic generation control
Generation = Demand + Losses	No change	No effect
Generation < Demand + Losses	Decrease	Load control/ Load shedding

Due to the scope of this research, we focus on third option only i.e., load shedding and will not be addressing the first two options further. In the literature, several methods are applied to overcome load shedding problem, which generally fall into three categories: demand-side management, conventional methods, and the integration of renewable and non-renewable sources, often referred to as HES. These methods along with their benefits and limitations are explained below.

A. DEMAND SIDE MANAGEMENT

Demand Side Management (DSM) optimizes energy consumption to enhance grid stability, influencing consumer behaviours to change load demand profiles [17], [18]. DSM traditionally serves as a strategy to delay expanding generation capacity, making it a short to medium-term solution for supply shortages. It achieves the change in the time, pattern and magnitude of utility's load to maintain generation margins and demand-supply balance of the system [19]. Measures within DSM include peak shaving and valley filling [20]. Customers are engaged through incentives and penalties, such as price-based and incentive-based programs, which encourage energy reduction during peak demand in return for financial incentives. Time-of-use pricing (TOU) is a common approach, charging higher rates during peak hours and lower rates during off-peak hours, known as indirect load control. While DSM schemes help address power shortage problems, their effectiveness in resolving load shedding is limited. They are best suited for immediate and short-term supply deficits. Long-term sustainability is challenging due to difficulties in predicting and encouraging consumer behaviours and maintaining incentives or subsidies. In cases of severe generation shortages, DSM is not a viable or effective solution.

B. CONVENTIONAL SOLUTION: DIESEL GENERATOR AND UPS/BATTERY

The diesel generator or battery-based UPS is the conventional solution to address the issue of load shedding. In this approach, the onus is on the customer to provide the energy resources to back-up the grid in the event of power cuts. For certain critical applications (hospital, military), the combined system, i.e., generator-UPS are also installed to ensure smooth power transition. Usually the capacity for generator and UPS system is sized according to the peak of the required load [21]. This solution is popular because system owners have control over mitigation strategies and associated costs. These resources are available 24/7 to combat load shedding [21], [22]. In Pakistan, 37% of domestic customers use UPS, while 44% rely on generators during load shedding [23]. Commercial customers also employ these solutions, with 64% using UPS and 51% using generators [24]. Besides, the impetus for using these sources is their low perceived costs, accessibility, and scalability. Due to the widespread adoption of generators and UPS, several studies have analysed their feasibility as an alternative solution for periods of power outage [24]. For instance, studies conducted in Lebanon [25], India [26] and Uganda [27]. Despite their simplicity, these solutions have drawbacks. UPS relies on grid electricity for charging, contributing to grid overloading and power quality issues, especially during peak hours. UPS power wastage can reach 25% during the charging and discharging process [28]. Generators have high running costs influenced by diesel prices and blackout hours, are noisy, require frequent maintenance, and have lower operational efficiencies. They also contribute to greenhouse gas emissions, harming the environment [29]. Due to these limitations, these solutions are not viable for long-term load shedding mitigation.

C. RENEWABLE BASED HYBRID ENERGY SYSTEM

With the growing concerns over the environmental impact of the fossil fuel, the trend is to incorporate the renewable and non-renewable energy sources (generators and batteries) with the grid [30], [31]. The HES is becoming popular, considering the significant drop in the price of PV modules and wind turbine hardware [32]. Additionally, it relieves the system from the vulnerabilities of fossil fuel cost and supply. In existing literature, HES have found applications including peak shaving [33], base-load power reduction [34], power quality enhancement [35], rural electrification [36], and provision for both cooling and heating [37]. For load shedding

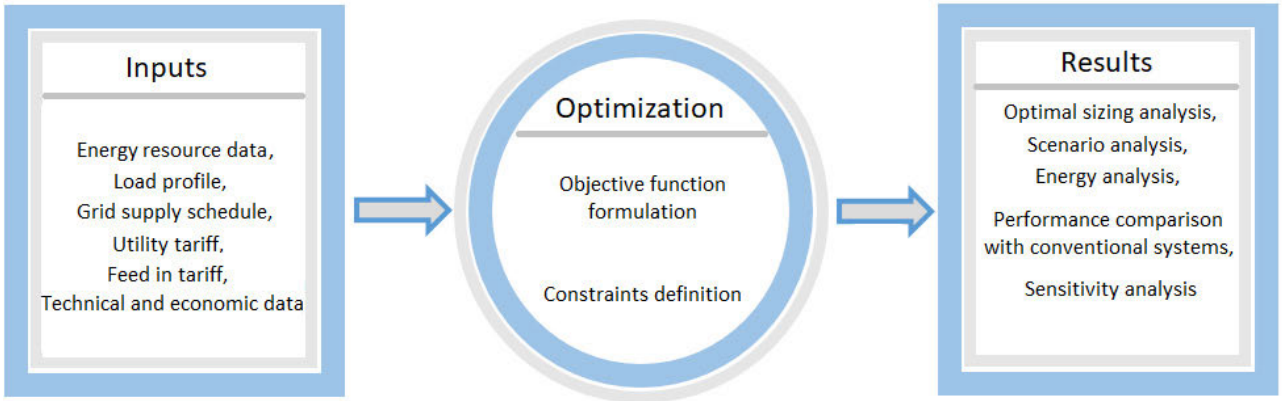

FIGURE 1. Research framework.

problem, besides satisfying the load demand during outage, the HES can provide several other benefits. For instance, the extra power from the renewables can be exported to the grid—thus, improving the performance and the reliability of the entire grid [38]. In addition, the HES provides a much quicker alternative for the network expansion, leading to a more sustainable supply for short and medium term [39]. From the economic perspective, the integration of renewables enables the prospect of feed-in-tarrif (FiT), and correspondingly offers monetary gains [40]. Considering these potential benefits, the HES can be considered as a more favorable option, compared to the two other load shedding solutions, i.e., DSM and conventional. However, to effectively utilize the resources, the HES must be optimally designed and operated. Yet, the existing literature lacks clarity on the cost of installing HES under load shedding conditions and the optimal operating conditions for the system.

III. RESEARCH METHODOLOGY

The research framework of this paper in three main parts is given in Figure 1. Inputs include potential energy technologies to be considered for HES along with their technical and economic specifications. Load profile, grid power supply schedule, utility tariff and feed in tariff (FiT) are also included.

The physical configuration of the HES proposed for this research is shown in Figure 2. The HES is linked to the utility grid at the point of common coupling (PCC). The arrows indicate the direction of power flow between the sources and the load. The principal sources within the HES are the PV and WT, while the batteries and diesel generators serve as backup sources. The HES operates in two main modes, grid mode and the islanded mode. The former is the normal system operation when utility grid supplies the load. During grid mode, RES (if available) will charge the BSU or alternatively inject surplus power to the grid. In the Islanded mode, HES sources (PV, WT, BSU and diesel generator) will directly supply the load during grid outage. The HES operation is realized with the help of power conditioning equipment i.e., dc/dc, dc/ac and ac/dc power converters. Equation 1 will govern the power balance of the system at any instant.

Optimization defines objective function and constraints for HES based on system's dispatch strategy. The two primary strategies are load following (LF) and cycle charging (CC) [41]. LF relies on (RES) to charge batteries, excluding diesel generators from this process due to high diesel costs. In contrast, CC permits generators to charge batteries after serving the load, taking advantage of low-load periods for generator shutdown. This paper employs a modified LF strategy that prioritizes RES for battery charging and also allows grid charging during off-peak hours. Finally, the result section provides multi dimension analysis. Sizing analysis presents optimal sizes of the sources involved and various economic metrics of the optimized system. Financial analysis describes the financial feasibility of the system by observing several budgeting metrics. Energy analysis focuses on reliability, total emissions, energy exchange with the grid, and the energy contributions of different sources, including their operation hours. Sensitivity analysis examines system performance in response to uncertainties in input or decision variables.

$$(P_{PV}(t) + P_{WT}(t) \pm P_{BSU}(t)\mathrm{x}\eta_{inv}) + P_{Gen}(t) \pm P_{Grid}(t) = P_{Load}(t) \quad (1)$$

here, $P_{Load}(t)$ represents the instantaneous load demand of the system while $P_{PV}(t)$, $P_{WT}(t)$, $P_{BSU}(t)$, $P_{Gen}(t)$ and $P_{Grid}(t)$ denote the power contribution of PV, WT, BSU, diesel generator and grid, respectively for the given time step. The η_{inv} represents the efficiency of the bidirectional inverter. The positive and negative sign attributed to BSU and grid signifies their capability to either generate or absorb power.

A. GOVERNING EQUATIONS OF HYBRID ENERGY SYSTEM

The performance of HES can be assessed using simulations based on the mathematical models of its sources. The appropriate models determine the amount of energy generated by each source for the given time step. The mathematical models are comprehensive for assessing system's performance under realistic conditions of varying operating scenarios.

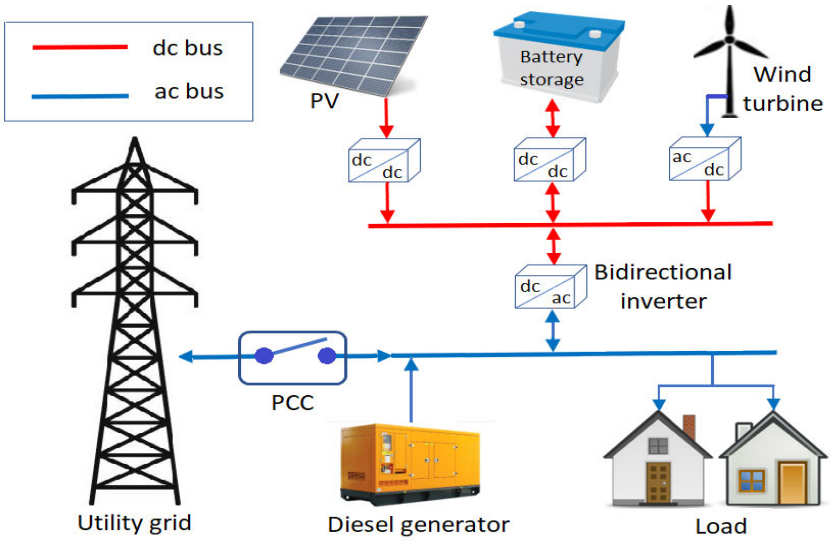

FIGURE 2. Proposed hybrid energy system.

1) PHOTOVOLTAIC POWER

PV panels convert solar energy into electricity during daylight hours, but they cannot generate energy at night. The output power of PV array can be calculated using single diode model where the output current is given as follows

$$I_{PV} = [(I_{SC-STC} + k_i(T - T_{STC}))\frac{G}{G_{STC}} - I_0[(e)^{\left(\frac{V_{PV}+I_{PV}R_S}{V_T}\right)} - 1](\frac{V_{PV} + I_{PV}R_S}{R_P}) \quad (2)$$

The I_{SC-STC} is the short circuit current at STC, k_i is the short circuit current at STC, k_i is the short circuit current coefficient given by the manufacturer, G is the cell surface irradiance whereas G_{STC} is the irradiance at STC and taken as 1000 W/m^2, T is the ambient temperature (in Kelvin), T_{STC} is the temperature at STC and considered 298K. V_T is the thermal voltage while R_S and R_P are the series and shunt resistances, respectively. The Newton-Raphson method is used to solve Equation (2) due to its transcendental nature. The iteration involves varying V_{PV} from zero to V_{OC}. The final V_{PV} is the voltage value at which maximum power (P_{PVMAX}) is extracted from the model, aligning with the concept of maximum power point tracking. The specifications of the selected PV panels are detailed in Appendix.

2) WIND TURBINE POWER

The output power of the WT is computed based on the wind speed-power characteristic curve as depicted in Figure 3. Depending on the wind speed (v), the curve is categorized into four regions. In region 1, when v is less than the cut-in speed value of the turbine ($v_{cut\ in}$), the power output is zero. Region 2 lies between $v_{cut\ in}$ and the rated speed (v_{rated}). Here, the WT starts to generate power and continuously increases as v increases. In Region 3, a constant output power (P_{rated}) is produced until the cut-off speed ($v_{cut\ off}$) is reached. Beyond $v_{cut\ off}$, the WT stops operating to protect its parts from high-speed winds and hence, no power is produced. This defines Region 4. The power generated by WT at a specific time t can be calculated according to [42] and given in Equation 3.

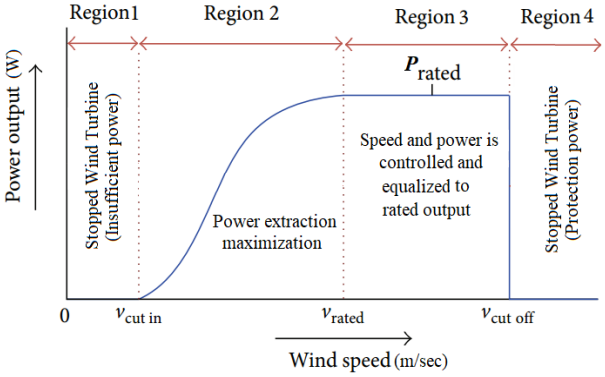

FIGURE 3. A typical WT wind speed power characteristic curve.

$$P_{WT}(t) = \begin{cases} 0 & v \le v_{cut\ in} \text{ or } v \ge v_{cut\ off} \\ P_{rated} & \left(\frac{v(t) - v_{cutin}}{v(t) - v_{cut\ in}}\right)^3 \ v_{cutin} \le v < v_{rated} \\ P_{rated} & v_{rated} \le v < v_{cut\ off} \end{cases} \quad (3)$$

To normalize the wind speed v (that is measured by an anemometer at a reference height H_0), to the designated hub height (H) of the WT under investigation, the following equation as employed in ([43] is used.

$$v = v_0 \left[\frac{H}{H_0}\right]^{\alpha} \quad (4)$$

Here, v (m/s) measured at H (m); v_0 is the wind speed calculated at the reference height H_0(m). The constant α is the ground surface friction coefficient; its value lies between [0.1, 0.25] [44].

3) BATTERY STORAGE UNIT POWER

The performance of BSU can be evaluated by the state of the charge (SOC) value at any time instant (t). The SOC increases when BSU charges and decreases as it discharges. However, an accurate SOC estimation protects battery units from being over charged or deeply discharged and thus, increases their life cycle [45]. This research utilizes coulomb (or ampere-hour) counting method for SOC estimation due to its simplicity. It tracks the instantaneous changes in SOC if the initial value of SOC is known. Figure 4 illustrates the concepts of SOC and depth of discharge (DOD) of the BSU [11], [46]. DOD indicates the percentage of the battery, which has been discharged in relation to fully charged state of the battery while the SOC refers to the amount of charge (Q_c) available in the BSU at a time (t) [47], i.e.,

$$SOC\,(t) = SOC\,(t-1) \times (1-\sigma) + (P_{Bat}\,(t)) \times \eta_{Bat} \quad (5)$$

Here σ denotes the hourly self-discharge rate, typically at 0.007% per hour [48]. However, for simplicity, we assume an ideal battery with σ set to zero. The parameter η_{Bat} accounts for the charging and discharging efficiency of the battery, and it is assumed to be 100% for both processes [49]. The term P_{Bat} represents the power for charging and discharging the battery unit based on the required and available power, respectively. To ensure battery longevity and safe operation, the SOC is constrained within specified upper and lower limits denoted as SOC_U and SOC_L.

The power required by BSU denoted as P_{Req} is the minimum amount of power such that if continuously applied over one time step Δt, it will raise the SOC of BSU from its initial level to the upper limit (i.e., SOC_U) in one time-step Δt. The P_{Req} is given as

$$P_{Req}\,(t) = \frac{(SOC_U - SOC\,(t)) \times C_{bat} \times N_{bat}}{\Delta t} \quad (6)$$

Likewise, the power available from BSU represented as P_{BSU} is the maximum amount of power that BSU can provide continuously without depleting its SOC to the lower limit (i.e., SOC_L) within a single time-step. The P_{BSU} is given as

$$P_{BSU}\,(t) = \frac{(SOC\,(t) - SOC_L) \times C_{bat} \times N_{bat}}{\Delta t} \quad (7)$$

In Equation (7), N_{Bat} refers to the total number of batteries in the BSU, while C_{Bat} signifies the nominal capacity for single battery (in kWh).

Initially, the BSU is assumed to be charged to 30%, with SOC_L at 10% and SOC_U set at 90%, as per [50]. According to the power dispatch strategy, the BSU discharges its energy (when needed) until it reaches its SOC_L level. Conversely, the BSU is charged until it reaches the SOC_U limit. However, the power exchange between the grid and the BSU is not solely dependent on surplus power availability and SOC level; it is also influenced by the TOU tariff of grid electricity.

4) DIESEL GENERATOR POWER

The primary role of a diesel generator is to serve as a backup power source. For the HES, the generator is employed as secondary back-up, in case when primary back-up (BSU) is unable to sustain the load. To enhance operational efficiency and reduce fuel consumption, the split 2-generator system, illustrated in Figure 5, is proposed. his dual-generator setup allows for the selection of the most suitable generator to closely match the specific load demand, preventing low operating efficiencies. Additionally, this configuration enhances system reliability and redundancy. In this setup, the first generator, Gen1, is smaller in capacity compared to the second generator, Gen2. These sizes are chosen carefully to ensure that both generators, when operating simultaneously, can meet the peak load requirements of the intended system. However, the generators are activated only when there is a need to cover energy deficits during load shedding intervals, i.e., when the PV, WT, and BSU cannot fulfill the load demand. The power produced by each generator can be described as:

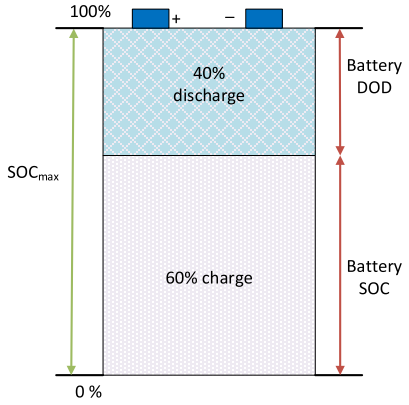

FIGURE 4. The concept of the battery SOC and DOD.

$$P_{Gen}\,(t) = P_n \times \eta_{Gen} \quad (8)$$

P_n represents the rated power in kilowatt (kW) provided by the manufacturer and η_{Gen} denotes the efficiency of the generator. Since the two generators are considered in this setup, total output power of the generators can be calculated as $P_{Gen}\,(t) = P_{Gen1}\,(t)_1 + P_{Gen2}\,(t)$.

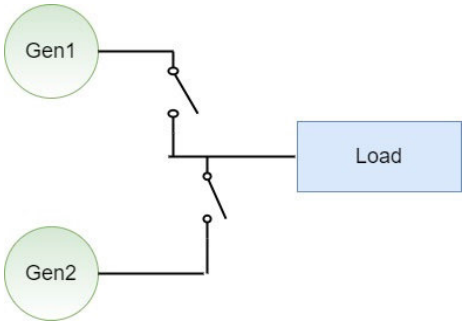

FIGURE 5. The split 2-generator system.

5) INVERTER POWER RATING

The inverter responsible for bridging the AC and DC sources in HES is characterized by its efficiency, denoted as η_{Inv}. The selection of inverter ratings is determined to accommodate

the maximum peak load, as indicated in [9]. This can be expressed as

$$P_{inv} = \frac{P_{Peak}}{\eta_{inv}} \tag{9}$$

P_{inv} represents the inverter power rating, P_{Peak} is the peak load demand from the system and η_{Inv} signifies the efficiency of the inverter.

B. CASE STUDY

To test the performance of proposed optimal design of HES, case study of Quetta city of Balochistan state in Pakistan is selected based on the following criteria.

- Actual power shortage scenario
- Availability of net metering plan
- Availability of load shedding and meteorological data

Balochistan, being the largest province of Pakistan in terms of land area (43%), faces various challenges when it comes to the provision of electricity. Historically, the region has been experiencing issues related to power shortages, load shedding, and inadequate electricity infrastructure. Due to the rugged mountains and sparsely populated areas, it becomes challenging to expand existing electricity network to fulfill increasing demand. Besides, most of the electricity relies on thermal sources, which is costly and less reliable compared to hydroelectric power in other parts of country. In order to manage the limited electricity supply and distribute it evenly among customers, hourly load shedding is a common practice in all districts of Balochistan. However, utility operators aim to minimize the inconvenience for users by announcing a daily power cut schedule in advance. Figure 6 illustrates the daily power supply schedule for the local distribution feeder in Quetta city, specifically on a summer day, June 14, 2020 [51]. The "off-states," as shown on the x-axis, represent the durations of load shedding. On this specific day, load shedding amounts to a total of 5 hours, distributed across three distinct time periods: from 6 to 8 hours, 13 to 15 hours, and 17 to 18 hours. It is important to note that this schedule varies throughout the year. On average, load shedding occurs for about 5 hours per day.

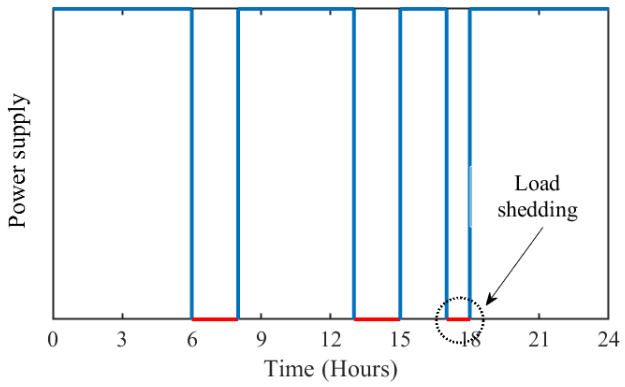

FIGURE 6. Grid power supply and outage schedule.

The energy consumption data of specific location is necessary to determine the load demand and the HES size. For this research, hourly load demand of small residential community having some public facilities is considered from [52]. Seasonal data shows higher energy consumption during the summer compared to the winter (see Figure 7). This is due to the hot weather and frequent usage of air conditions in the region. The daily consumption during summer and winter is 345 and 309 kWh, respectively. The peak power usage is noted to be 26.66 and 23.91 kW, respectively. The electricity price in this location consists of two TOU tariff (on peak and off peak). On peak (13.1 cents/kWh) consists of four hours from hours 18 to 22. The remaining twenty hours is the off peak (9.3 cents/kWh) from 22 to 18 hour.

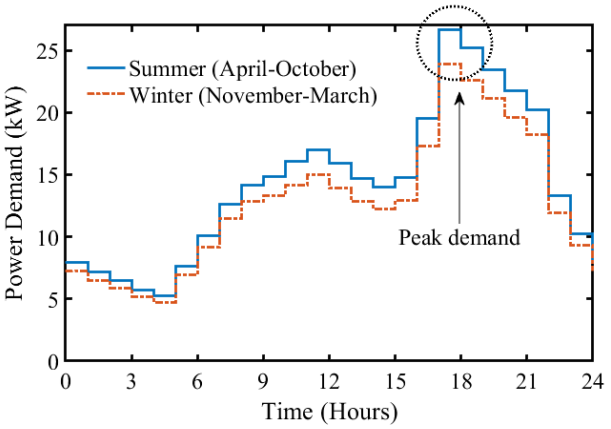

FIGURE 7. Seasonal load demand of residential community on hourly basis.

C. OPTIMIZATION OF HYBRID ENERGY SYSTEM

Optimization in this work aims to minimize the cost of electricity and the payback time of the HES investment while maximizing the reliability of the system. Assessing the cost and payback time helps determine the economic and financial feasibility of the HES, while the reliability evaluates its technical performance. However, these objectives often conflict with one another. For instance, system reliability increases if HES is oversized but it also inflates the overall system cost. Conversely, under size HES can result in reduced reliability. Thus, finding the tradeoff among these objectives is a key challenge in this work. To address this, our optimization framework combines the optimal sizing of components with the power dispatch strategy of the system, primarily following the LF strategy, with some necessary modifications for grid-connected architecture, as depicted in Figure 8. The implementation of the optimization method is performed using three well known metrics namely: levelized electricity cost (LEC), payback period (PBP) and the loss of power supply probability (LPSP). These metrics are briefly explained below.

1) LEVELIZED ELECTRICITY COST

The LEC is commonly utilized metric to evaluate the cost of electricity of a particular power generation source. LEC provides a standardized way of comparing the costs of different energy technologies of different project size, lifetime, capital

cost, return, risk, and capacities [53]. The LEC is calculated as

$$LEC = \frac{Total\ System\ Cost}{Total\ Energy\ Production} = \sum_{n=1}^{N} \frac{Cost_{System}/(1+r)^n}{Energy_{System}/(1+r)^n} \left(\frac{\$}{kWh}\right) \quad (10)$$

here $n = 1$ represents the first year (beginning) of the project while N refers to the project lifetime and r shows the discount rate [54]. The total system cost ($Cost_{System}$) includes three main components: 1) the initial cost (investments) of the assets, 2) the operating cost (insurance, running, repairs) over the project lifetime and, 3) the replacement cost of defected assets.

2) PAYBACK PERIOD

The LEC mainly focuses on the cost of electricity production, it does not take into account the revenue opportunities [55]. On the other hand, the PBP considers both the cost and the revenue of the system, making it a critical factor for conducting a comprehensive life-cycle analysis and evaluating the financial feasibility of the project [56]. The PBP is defined as the time (in years) in which a project may reach its breakeven point. The PBP in The PBP in simplified form is calculated as [57].

$$PBP = \frac{Costs_{System}}{Annual\ Revenue} \quad (11)$$

The $Costs_{System}$ are the total costs of system over its lifetime. Likewise, the *Annual revenue* represents the yearly amount of revenue generated from selling energy produced by HES.

3) LOSS OF POWER SUPPLY PROBABILITY

Among several technical metrics, LPSP is widely used parameter to assess the reliability of PV and WT due to their intermittent behavior. It is defined as the probability of system to experience a loss of power supply for the required load over a given time frame [58]. It can be expressed as

$$LPSP = \frac{\sum_{t=1}^{T} LPS(t)}{\sum_{t=1}^{T} P_{Load}(t)} \quad (12)$$

$$LPS = P_{Load}(t) - (P_{PV}(t) + P_{WT}(t) + P_{BSU}(t)) \times \eta_{inv} \quad (13)$$

where T represents the complete time horizon of the analysis while the $t$shows the current time step. In case of HES, LPS represents the loss of power supply when the energy produced by the renewables and that stored in the BSU are not sufficient to supply the load. The value of LPSP lies in the range of 0 to1. A value of 0 indicates that the load demand is fully satisfied, while a value of 1 signifies that the demand is not satisfied at all. It should be noted that in case of LPSP > 0, diesel generator will be activated to fulfill the remaining load.

D. OBJECTIVE FUNCTION FORMULATION

The LEC, PBP and LPSP play a significant role to solve optimization problem of HES. The LEC and PBP are economical metrics while LPSP is the technical metric. By employing the weighted sum method to incorporate multiple objectives into a single combined objective, the optimization function of the HES as a minimization problem is formulated as:

$$minJ\left(n_p\right) = \sum\nolimits_t \min\left(W_1 LPSP + W_2 LEC + W_3 PBP\right) \quad (14)$$

The weighting coefficients W_1, W_2, and W_3 correspond to each criterion and represent the normalization process. The normalization is required to remove the influence of objectives due to the different magnitudes [59]. The variable n_p is the sizing vector: $n_p = \{N_{PV}, N_{WT}, N_{Bat}\}$, where N_{PV}, N_{WT} and N_{Bat} is the number of PV, WT and battery units, respectively. The idea is to discover an optimized combination of PV modules, WT units, and BSU batteries that can achieve the lowest value of the defined objective function while adhering to the given system constraints. In other words, the optimization process of HES is subjected to following design and operation constraints.

E. CAPACITY LIMIT CONSTRAINT

Capacity limit constraint is related to design of HES. This constraint decides the boundary for the decision variables such that their values should lie between upper and lower limits

$$n_p = \text{integer}, n_p^{min} \le n_p \le n_p^{max} \quad (15)$$

where $n_p \in \{N_{PV}, N_{WT}, N_{bat}\}$, shows the number of components of PV, WT and batteries. The boundaries are set on hit and trial method in all optimization algorithms. The bounds are used to reduce the convergence process.

F. BATTERY OPERATION CONSTRAINT

This constraint defines BSU charging and discharging conditions based on the level of SOC. To minimize the ageing process of BSU, its SOC should remain between upper (SOC_U) and lower (SOC_L) limit [60]. Besides, Renewables (PV, WT) will charge BSU when there is surplus power at any time. However, grid will charge BSU during the off-peak periods only. This will not only avoid high costs of BSU charging operation but also maximize indigenous renewables utilization. Similarly, BSU will discharge when power from PV and WT is not sufficient to meet the load. The BSU will supply deficit load during the islanded mode. These constraints are formulated by Equations (16) to (20).

$$SOC_L \le SOC(t) \le SOC_U \quad (16)$$

$$PV_{Ch\ BSU} = P_{PV}(t) - P_{Load}(t) \text{ for all} \quad (17)$$

$$WT_{Ch\ BSU} = P_{WT}(t) - P_{Load}(t) \text{ for all } t \quad (18)$$

$$Grid_{Ch\ BSU} = P_{Grid}(t) - P_{Load}(t) \text{ for } t = \text{Off-peak hours} \quad (19)$$

$$BSU_{Disch} = P_{LoadDef}\ (t) \quad \text{for } t = \text{Islanded mode} \tag{20}$$

G. GRID INJECTING CONSTRAINT

In order to support grid operation and to take economic benefits, the surplus power from RES will be injected under the following constraints.

$$PV_{inj\ Grid} = P_{PV}\ (t) - PV_{ch\ BSU}\ (t) \quad \text{for } t = \text{Islanded mode} \tag{21}$$

$$WT_{inj\ Grid} = P_{WT}\ (t) - WT_{ch\ BSU}\ (t) \quad \text{for } t = \text{Islanded mode} \tag{22}$$

H. GRASSHOPPER OPTIMIZATION ALGORITHM FOR HES SIZING

The GOA is inspired from the grasshoppers' movement patterns as they naturally search for food in their environment. The mathematical expression representing the swarm behavior of grasshoppers according to [61] is given as:

$$P_i^d = c\left[\sum_{\substack{j=1\\ j\neq i}}^{N} c\frac{ub_d - lb_d}{2} S\left(\left|P_j^d - P_i^d\right|\right)\frac{P_j - P_i}{d_{ij}}\right] + \hat{T}_d \tag{23}$$

The P_i and P_j show the positions of i^{th} and j^{th} grasshopper while ub_d and lb_d refer to their upper and lower bounds in the d^{th} dimension space, respectively. d_{ij} represents the distance between i^{th} and the j^{th} grasshopper and S denotes the social interaction between them. During the search process, S is regarded as the most significant component to influence the movement of the grasshoppers. $\hat{T}_d$ shows the targeted/ best value of the d^{th} dimension. The coefficient c plays a crucial role in defining the comfort region, repulsion region, and attraction region of the grasshoppers. It is utilized twice to facilitate the deceleration process in these creatures. The first instance of c reduces the search region in correlation with the number of iterations, while the second c lessens the impact of attraction and repulsion forces among the grasshoppers. To enhance the balance between exploration and exploitation in relation to the number of iterations, the value of c is updated using Equation 24.

$$c = c_{max} - t\frac{c_{max} - c_{min}}{t_{max}} \tag{24}$$

here c_{min} and c_{max} are the minimum and maximum values of c, respectively. t is the current iteration, while t_{max} represents the maximum iteration. Each grasshopper's position is updated based on three key factors: its current position, the global best position within the swarm, and the positions of other grasshoppers in the same swarm. This avoids local trapping during the optimization process. In this work, GOA solves the optimization problem by finding best sizes of HES components. As the simulation starts, GOA selects random particles from the search landscape whose boundaries are set by the user. The particles navigate the search landscape by following the algorithm's governing equations, aiming to optimize the defined objective function. The proposed optimization framework integrated with power dispatch strategy of the HES is depicted in Figure 8. The optimization process continues until the preset stopping criteria are met, at which point the algorithm concludes.

IV. RESULTS AND DISCUSSION

The optimization framework of HES is simulated in MATLAB. Several settings are defined for the simulations. System operation is based on the LF strategy, in order to optimize the utilization of RES. The project lifespan is set for 25 years. The chosen components of HES and their technical and economic parameters are given in Table 7 in Appendix. These parameters are assumed to be constant throughout the analysis. Besides, the utilized data i.e., load profile, load shedding schedule and the weather resource data (irradiance, wind speed, temperature) are assumed to be known with certainty throughout the project lifecycle. The annual weather data of FY 2020 of the studied location downloaded from public repository named Solcast is used [62]. The hourly energy resource data is used due to its widespread acceptance in long-term system assessment. while, it also enables quicker computational processing compared to datasets with higher resolutions. To reflect the real-world conditions, discounted energy and the degradation rate are also included in the calculations. Moreover, the effects of uncertainty are checked using sensitivity analysis in the last section.

A. OPTIMAL SIZING ANALYSIS

Since the correct sizing of the HES is very crucial to ensure its efficient operation, two optimization algorithms, namely the GOA and PSO are used to find the best combination of its components. The decision variables are optimum number of photovoltaic modules (N_{PV}), wind turbine (N_{WT}) and batteries (N_{Bat}) in BSU. The optimization process is subjected to the following search ranges. The search space is defined to speed up the convergence process and to avoid unwanted solutions while ensuring the consideration of all variables. It is important to mention here that first the objective function is solved using the GOA, while PSO is applied for benchmarking purposes. The source codes of GOA and PSO are taken from [63] and the following parameter settings are considered during simulation

- GOA: Population size: $n_p = 20$, shrinking factor parameters: $C_{min} = 0.00001$ and $C_{max} = 1$, intensity of attraction: $f = 0.5$ and $l = 1.5$, maximum number of iterations performed: $i = 100$.
- PSO: Population size: $n_p = 20$, inertia weight: w = 0.9, acceleration coefficients: $C_1 = 2$, $C_2 = 2$, maximum number of iterations performed: $i = 100$.

$$\text{Variable range} \begin{cases} 10 < N_{PV} \leq 110 \\ 2 < N_{WT} \leq 15 \\ 5 < N_{Bat} \leq 20 \end{cases} \tag{25}$$

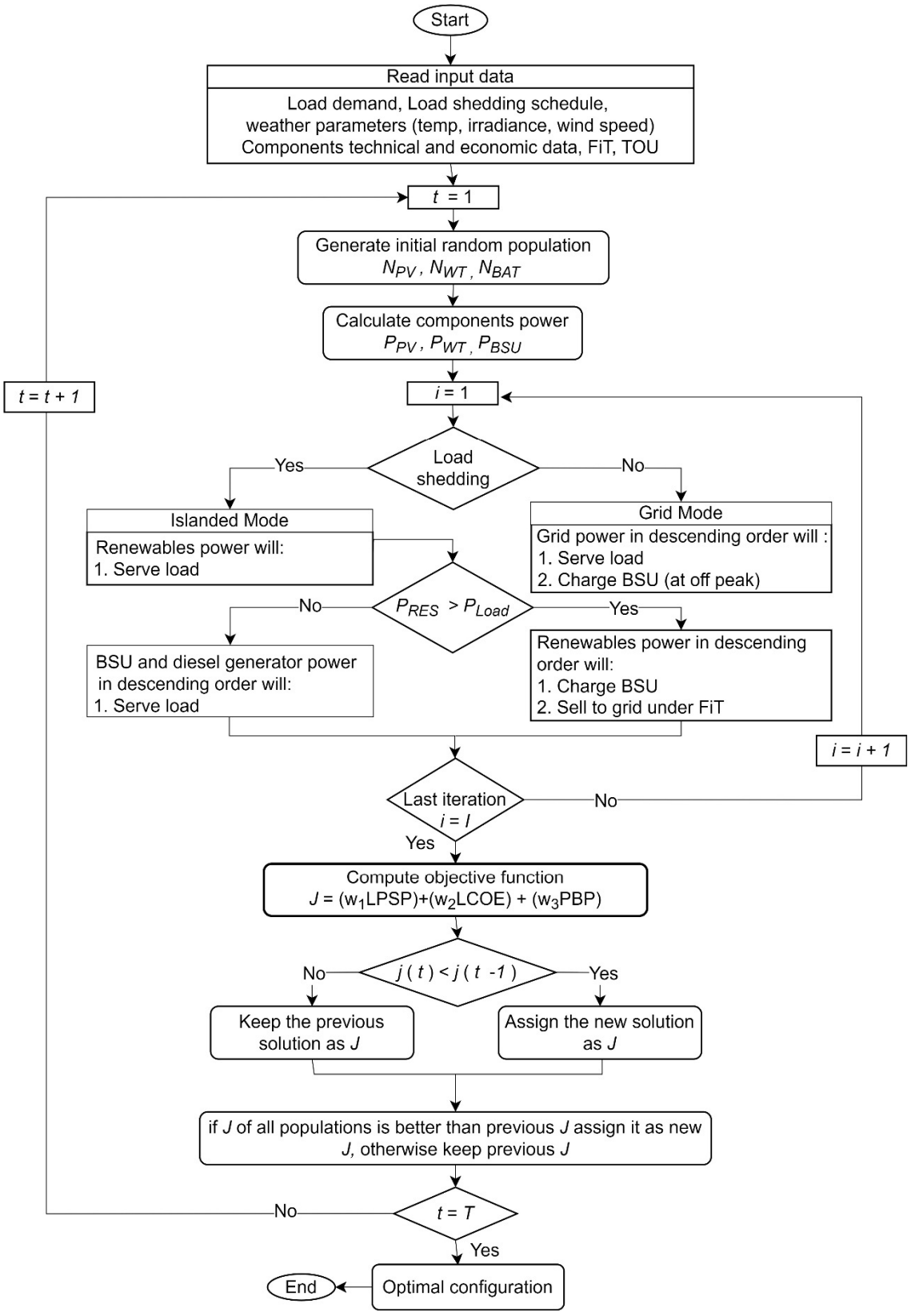

FIGURE 8. Complete optimization process of hybrid energy system.

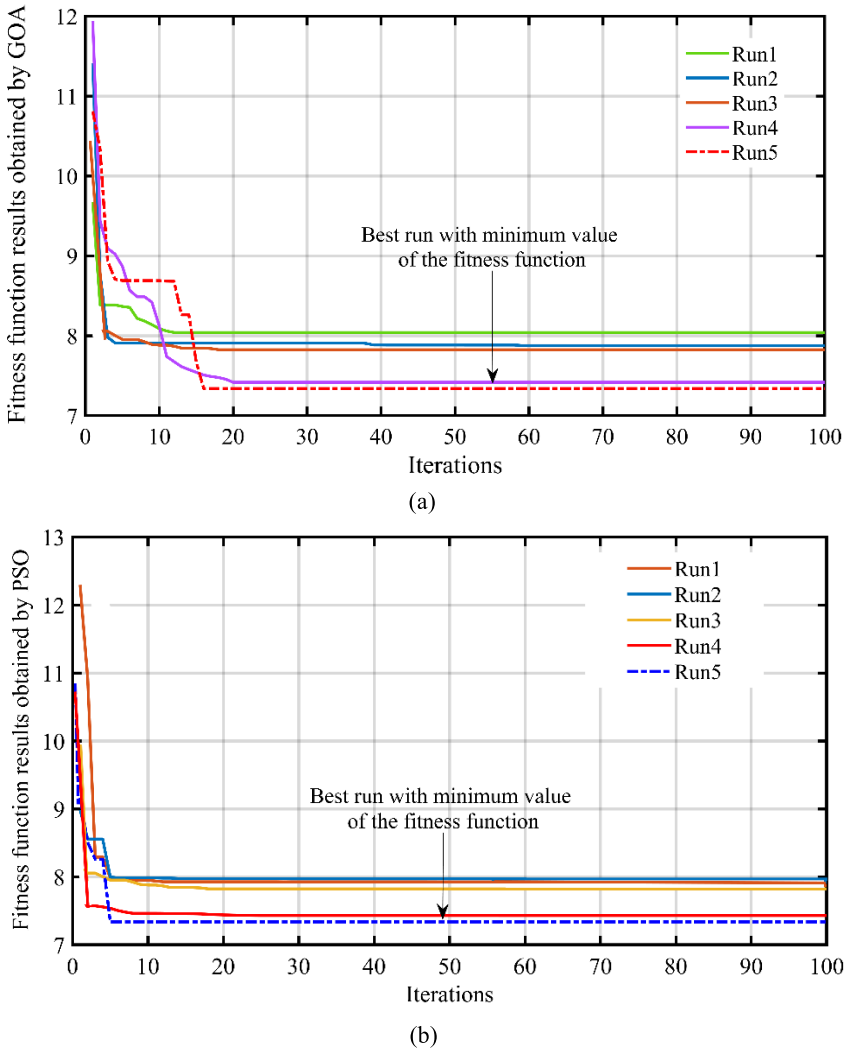

FIGURE 9. The convergence of algorithms (a) GOA and (b) PSO.

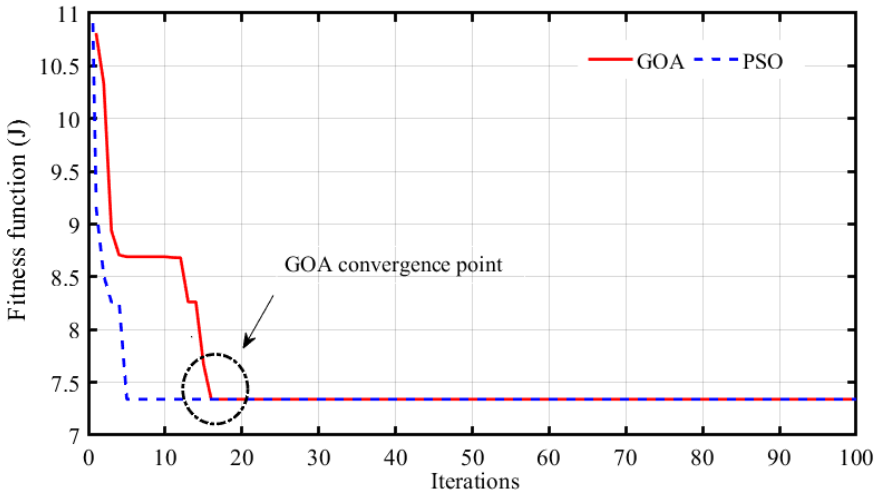

FIGURE 10. The best convergence curves of GOA and PSO.

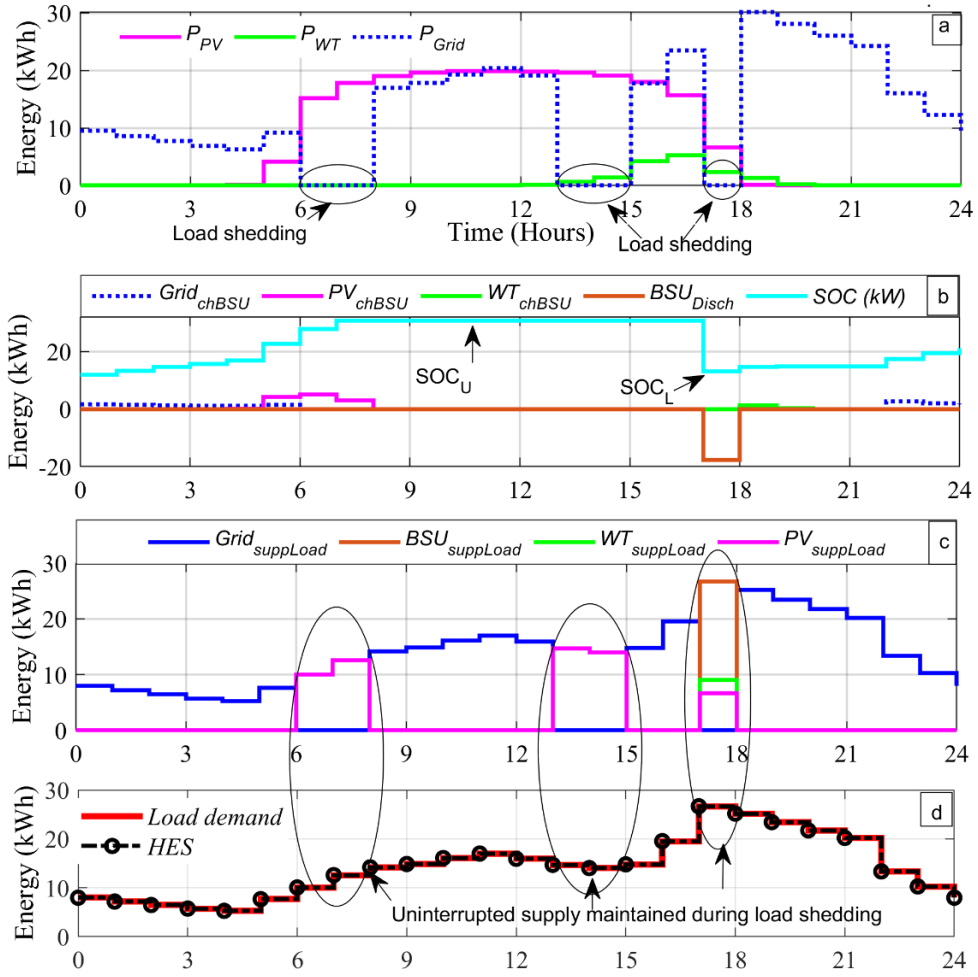

FIGURE 11. Operation of HES during sunny day (14th June 2020). (a) Available power from grid, PV and WT. b) BSU operation during charging and discharging. (c) Integrated operation of Grid, PV, WT and BSU. (d) The resiliency of HES in sustaining the load.

Since the population-based algorithms converge stochastically, the outcome of single run may not provide conclusive results. Therefore, GOA and PSO are simulated multiple times and their best 5 runs are displayed in Figure 9 part a and b, respectively. The goal is to minimize the objective function, hence the run with the lowest value signifies the best result. For GOA, the optimal solution is indicated by the red dashed curve (as referenced in Figure 9 (a), resulting in the objective function (J) value of 7.4. In contrast, for PSO, the best outcome corresponds to the blue dashed curve in Figure 9 (b). A direct comparison of the optimal curves from both algorithms is presented in Figure 10. Notably, both algorithms converge to an approximately identical fitness value ($J = 7.4$), indicating the selection of the same configuration of PV, WT, and battery installations. These findings affirm the accuracy and reliability of the optimal sizing outcomes. However, it's worth noting that the PSO algorithm exhibits faster convergence, achieving this outcome by the 5th iteration.

The LEC obtained for the optimal configuration of HEC components is 6.64 cents/kWh, indicating that it is less than grid electricity per unit cost (9.3 cents/kWh), highlighting the economic potential of HES. The LPSP value of 0.0092 is achieved falling within a satisfactory range on the scale of 0 to 1. A value of 0 indicates that the load will always be met by the given configuration, ensuring continuous power supply, while a value of 1 implies that the load will never be satisfied, posing reliability issues in meeting the electricity demand. Consequently, the PBP is calculated to be 7.4 years, making it an appealing proposition for the investors when considering the 25 years life span of the HES project.

Based on the obtained optimal configuration and the considered technical parameters (given in Table 7), designed HES includes PV array with a rating of 35.75 kW, WT with a rating of 10 kW, and a BSU with a rating of 28.8 kWh. Additionally, the diesel generator of 30kWp is included as backup source. Once optimal configuration of HES is determined, its performance can be assessed and compared with other existing options.

B. SCENARIO ANALYSIS

The performance of HES is tested on a typical sunny and cloudy day. The selection of these scenarios is deliberate,

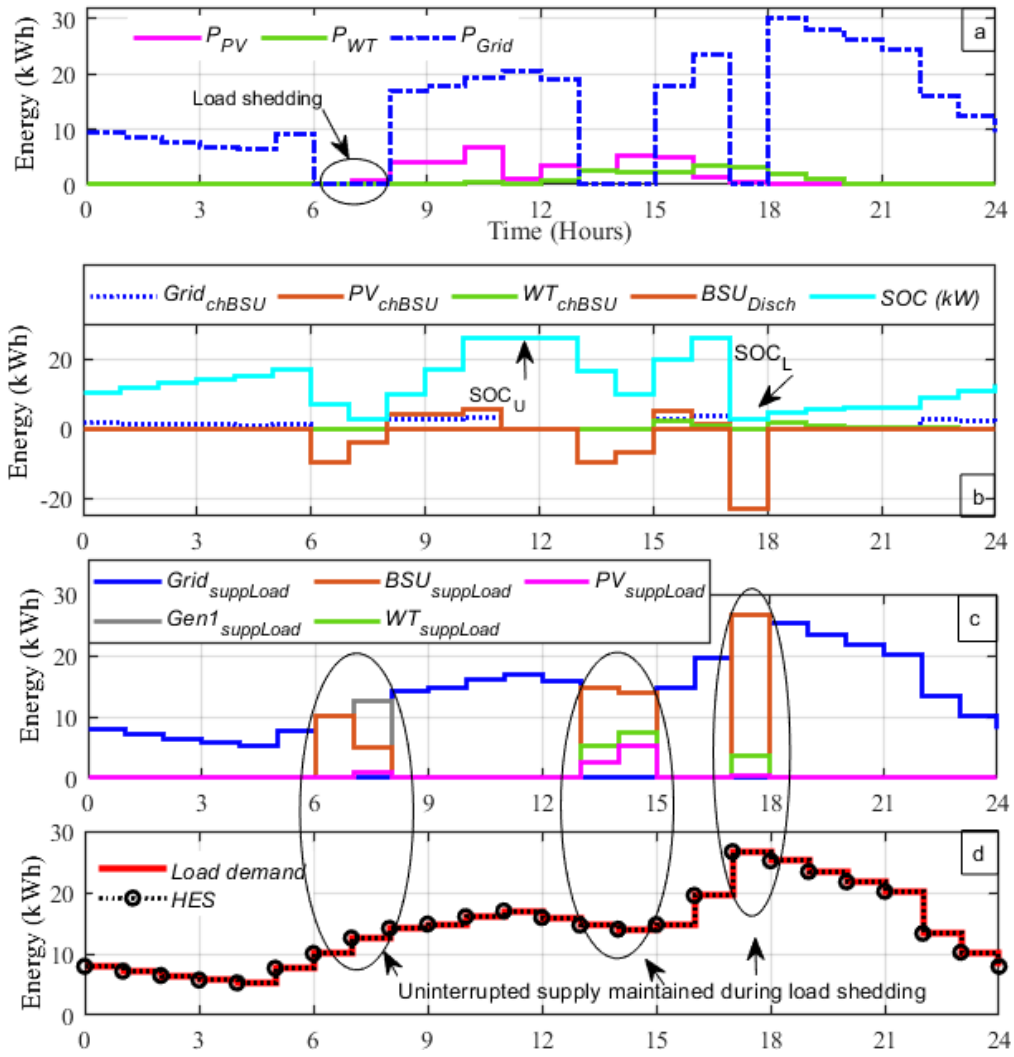

FIGURE 12. Operation of HES during sunny day (14th April 2020), (a) Available power from grid, PV and WT, b) BSU operation during charging and discharging, (c) Integrated operation of Grid, PV, WT and BSU, (d) The resiliency of HES in sustaining the load.

TABLE 2. Annual recorded carbon emissions of optimal installed capacities of different systems.

System	Installed capacity (kW)				CO_2 emissions (Kg/year)
	PV	WT	Batteries	Generator	
HES	35.75	10	28.8	30	503
Generator (system1)	--	--	--	30	7423
UPS (system2)	--	--	34.2	--	0
Generator-UPS (system3)	--	--	18.0	30	3994

aiming at assessing system's reliability under different operating conditions. The operational snapshots of HES for these days are shown in Figure 11 and Figure 12, respectively. The simulations are performed for the load demand given as Figure 8. The results are presented in four plots. Plot (a) displays the available power status of specific day, indicating the contributions from grid (P_{Grid}), PV (P_{PV}) and WT (P_{WT}). Plot (b) illustrates the charging and discharging patterns of BSU along with the corresponding SOC variations. In plot (c), the energy transactions between various sources,

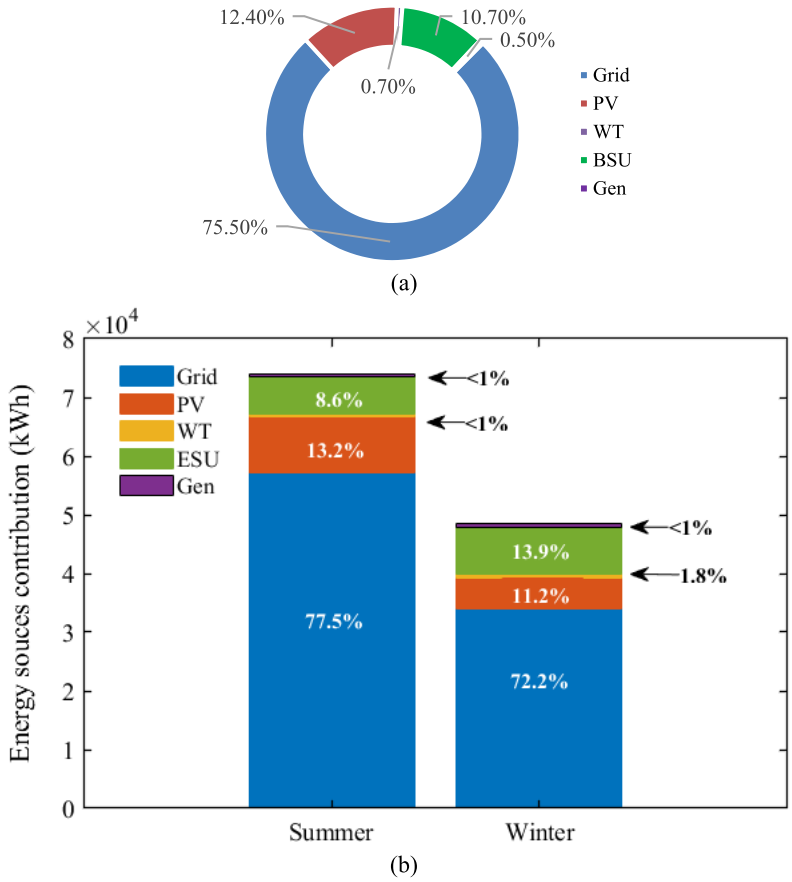

FIGURE 13. Contribution of different energy sources a) yearly basis and, b) seasonal basis.

including grid, PV, WT, BSU and generators (if utilized) are visualized. Finally, plot (d) demonstrates the power delivered by the HES in response to the load demand of this specific day. If the power profile closely follows the contour of the load demand, it is assumed that the system is reliable.

As can be observed from the grid supply (P_{Grid}) in Figure 11 (a) and Figure 12 (a), load shedding is imposed for five hours, divided into three separate trenches, i.e., hours 6-8, 13-15, and 17-18. During the absence of the grid power, the HES sources, i.e., PV, WT, BSU and generator supply the required load. HES shows remarkable resilience during both sunny and cloudy days. Despite outage from the grid, the HES can maintain the power availability and that also with minimum utilization of the generators.

C. ENERGY ANALYSIS

The energy contribution of different sources over one-year HES operation is analyzed. The annual energy demand of the system is 120,610 kWh. Out of this, 91,055 kWh (or 75.5% of the total energy) is derived from the grid. The energy deficit during grid outage is partly resolved by the PV (14,999 kWh or 12.4%) and WT (960 kWh or 0.7%). In addition, the BSU discharged 12,960 kWh (or 10.7%) to meet the load. Based on the data, the major energy sources contributing are the PV and BSU (23.1%). To maintain the power balance, generator contributed 636kWh (0.5%) to the load. However, the generator set produced total energy of 1861kWh. This is because the generators are designed at the maximum load demand. The carbon emissions from diesel are recorded as 0.27 kgC_{O2}/kWh [64]. Thus, a total of 1861 kWh would result in approximately 503 kgCO2 annually. Figure 13 displays contribution of different sources of HES to supply required load demand.

D. PERFORMANCE COMPARISON WITH CONVENTIONAL SYSTEMS

The performance of HES is compared with three systems: standby diesel generator (system 1), online UPS (system 2) and combination of both i.e., generator and UPS (system 3). System1 consists of two generators with same specification like HES i.e., Gen_1 (10kW) and Gen_2 (20kW) are considered. Total generator set size is determined by the peak demand of the system. For system 2 with UPS, $N_{Bat} = 19$, while for system 3, i.e., the combined UPS-generator system, $N_{Bat} = 10$ are employed. The N_{Bat} for system 2 and system 3 are optimized with the help of GOA. The sizes are selected according to minimum value of the LEC and PBP while fulfilling the load requirement (as shown in Figure 8). To ensure

TABLE 3. The cost analysis and payback period of considered systems.

System	Capital costs ($)	O&M costs ($)	Total costs ($)	LEC (cents/kWh)	PBP (years)
HES	25,559	14,325	39,884	6.64	7.4
Generator (system1)	5,000	108,661	113,661	29.68	12.9
UPS (system2)	6,419	40,741	47,160	13.23	9.8
Generator-UPS (system3)	91,69	68,370	77,539	19.82	11.3

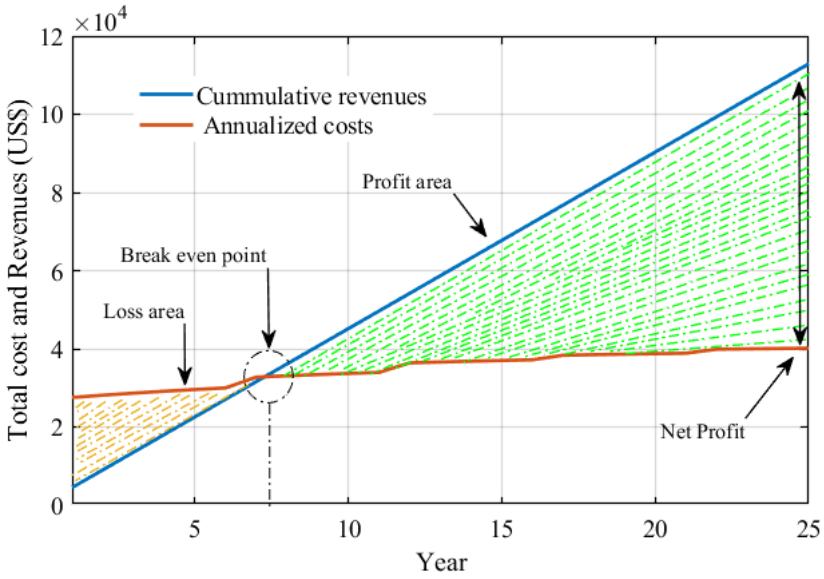

FIGURE 14. Payback period and profit analysis of HES over lifecycle.

fair comparison with HES, these systems are simulated using same load and load shedding profiles.

The annual performance of these systems considering the generator emission is given in Table 2. The HES has a yearly operational duration of 190 hours for its generators. In contrast, when using standalone generators (system 1), they need to be active for 1,678 hours. However, when combined with UPS (system 3), the generator runtime is reduced to 1,160 hours. This important benchmarking proves the superiority of HES in comparison to the conventional systems. For the latter, the generators must be turned on at every grid power outage occurrence to ensure supply availability. The main impetus to condense generator utilization is the savings in the (diesel) fuel cost and to reduce emissions. From the results, it is clear that the inclusion of renewable sources in HES significantly reduces fuel consumption of generators. Given the economic aspects are the primary factors during system design, a thorough economic analysis of all systems is required. The LEC for the conventional systems is calculated based on 25 years system lifetime like HES. Throughout the analysis, same discount rate (9%) and diesel price (69 cents/L) are considered.

The LEC and PBP for all systems are calculated using Equations (10) and (11). Accordingly, the annual income for HES and conventional systems can be calculated as $Annual\ Income_{HES} = Total\ Energy\ Contribution_{RES} \times FiT$, $Annual\ Income_{Con\_Sys} = Total\ Energy\ Contribution_{Con\_Sys} \times LEC_{Con\_Sys}$, respectively. Table 3 presents important financial information of the considered systems.

E. PAYBACK PERIOD AND PROFIT ANALYSIS

The profitability assessment of the HES is conducted based on its PBP. To reinstate, the PBP is calculated by dividing the total project costs with the annual income of the system. The latter is dependent on the yearly share of renewable energy eligible for the FiT. Note that the FiT is a favorable price given to RES generators for supplying surplus energy to the grid. In this study, the FiT applies when RES (PV, WT) supply the load during grid power outage intervals or when inject to the grid. The FiT price used in the case study is 12 cents/kWh,

TABLE 4. Economic comparison of HES with existing studies.

Reference and Year	Potential Sources and System Configuration	Location	LEC (cents/kWh)	PBP (Years)
[64], 2022	PV, WT (Grid-connected)	Saudi Arabia	6.1	20.7
[65], 2022	PV, WT, BSU, Gen, Hydrogen storage (Standalone)	Turkey	37.6	4.11
[66], 2022	PV, WT, BSU, Gen (Standalone)	Philippines	36.4	14.1
[67], 2022	PV, BSU, Gen (Standalone)	India	19.6	3.5
[68], 2023	PV, Gen (Grid-connected)	Bangladesh	2.2	6.95
[69], 2022	PV, WT, Gen (Grid-connected & Standalone)	Italy	10.9 (GC), 5.3 (SA)	3.53 (GC), 6.2 (SA)
Proposed	PV, WT, BSU, Gen (Grid-connected)	Pakistan	6.6	7.4

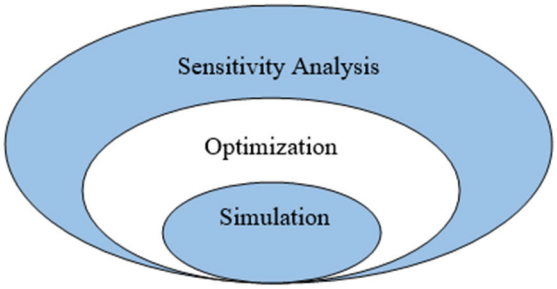

FIGURE 15. Relationship among simulation, optimization and sensitivity analysis.

TABLE 5. Different scenarios for sensitivity analysis.

Category	Deviation	Observations
Economic parameters	±10%, ±20%	Diesel price, PV price, WT price, Battery price, FiT
Climatological parameters	± 10%, ±20%	PV power, WT power, BSU capacity
Demand profile	±10%, ±20%	Load demand

which is based on the approved FiT in Pakistan. To aid in comprehension, Figure 14 displays the annualized costs and revenue flow of the HES. The linearity of the revenue curve is due to the assumption of constant load demand throughout the project's life cycle.

Conversely, the non-linearity of the annualized cost curve arises from the discounted and replacement costs of HES components. These replacements, such as batteries and inverters, must be made at different intervals during the project's lifespan. The cumulative annualized costs encompass the capital costs and adjusted operation and maintenance (O&M) costs incurred over time. As can be observed, the total annualized costs over the HES lifespan of 25 years, align with the total costs of HES designed configuration, amounting to USD 39,884. The profit loss breakeven point is reached at 7.4 years, beyond which the project begins generating profits. Over the remaining project lifetime, the net profit sums up to approximately USD 75,000.

F. COMPARISON WITH PREVIOUS WORKS

Comparing the performance of proposed HES with existing studies is challenging because there are no notable studies focusing on HES configuration for load shedding problem. However, The LEC and PBP of the HES obtained in the existing studies compared. Table 4 presents these metrics from various studies, highlighting HES competitive performance, confirming the effectiveness of adopted. method. The variations in LEC and PBP values in the table result from the complex interaction of multiple factors which emphasize the need for sensitivity analysis to identify influential parameters.

G. SENSITIVITY ANALYSIS

The sensitivity analysis is performed to observe the system performance with respect to the uncertainty or variations in certain input or decision variables. Figure 15 illustrates the relationship between the simulation, optimization, and sensitivity analysis. The optimization oval (circle) encloses the simulation oval to represent the fact that a single optimization consists of multiple simulations runs. Similarly, the sensitivity analysis encompasses optimization oval—which implies that a single sensitivity analysis consists of multiple optimizations runs. The analysis is performed using three different categories of parameters as provided in Table 5.

1) ECONOMIC PARAMETERS

To evaluate the impact of equipment cost on the HES design, the changes in cost of PV panels, WT and batteries are done in four increments: −10%, −20, +10% and +20%. In addition, the change in diesel fuel price is also considered. The sensitivity analysis using simplified line charts carried out in relation to LEC and PBP are shown in Figure 16. The lines in the charts can quickly highlight the variables

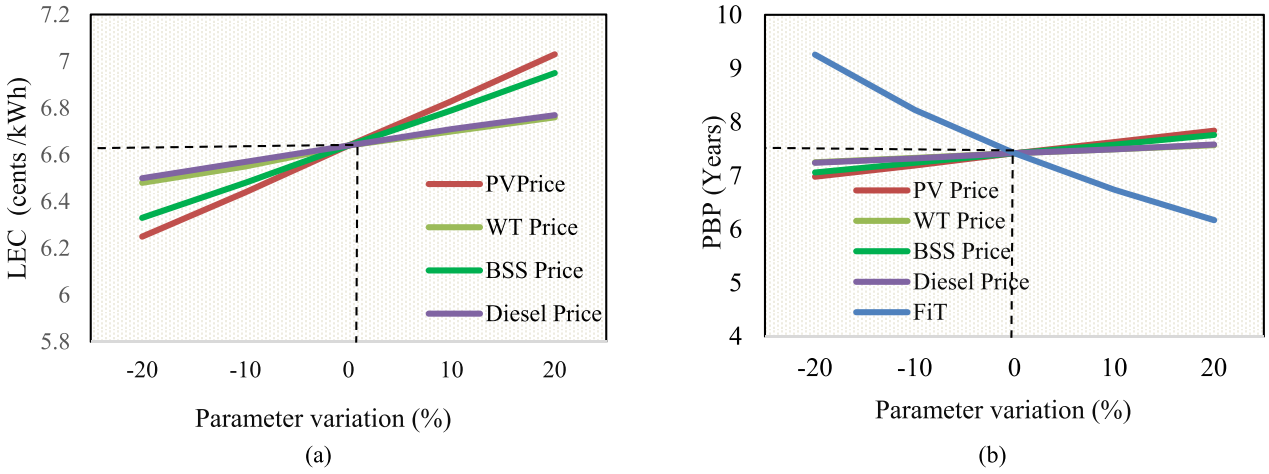

FIGURE 16. Impact of economic parameters on the LEC and PBP of HES.

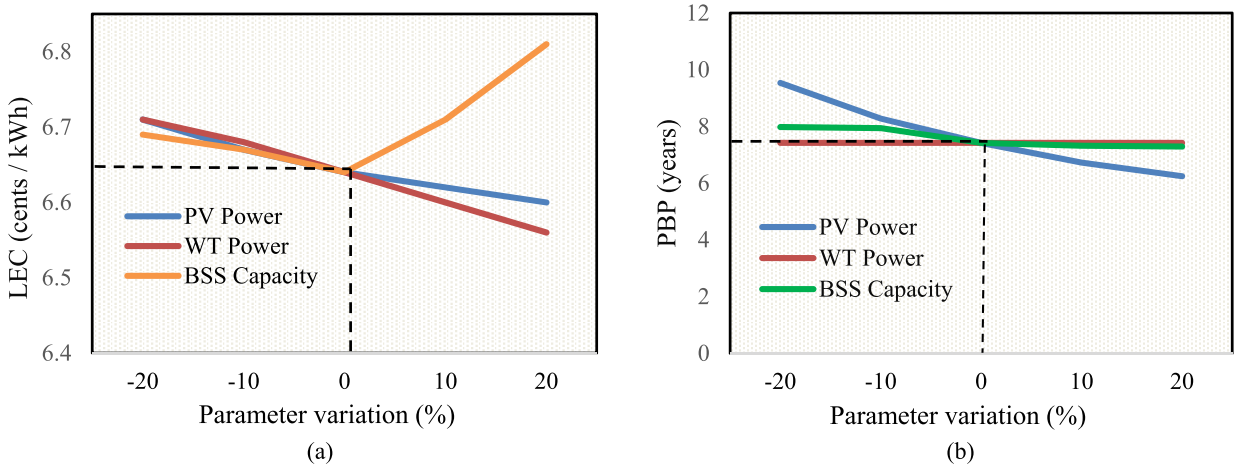

FIGURE 17. Impact of climatological parameters on the LEC and PBP.

that are most/least sensitive to variations. The procedure is straightforward: the specific variable of interest is varied to uncertain values while all other variables are held constant.

This allows testing the degree to which the result is sensitive to the specified variable. The ''zero point'' on the abscissa refers to the optimized value of LEC and PBP of HES, i.e., 6.64 cents/kWh and 7.4 years.

In plot (a), the LEC increases with the increase in the equipment cost and vice versa. Among the variables, the capital cost of PV (PV price) is the main driver of the LEC variation, followed by the battery price. On the other hand, the diesel price has a reduced impact despite being the subsystem with the largest operational cost while the WT having the least impact.

This is because of the least contribution of these sources for the optimal operation of the HES. In plot (b), the impact of equipment cost and diesel price against the PBP of the HES is examined. Since the FiT influences the PBP of the system, its variation is considered too. Figure 17 (b) shows the resulting PBP sensitivity plots, with the zero-percentage indicating 7.4 years. As expected, the increase in component prices increases the PBP. Among the components, PV has the major impact followed by the battery cost. Note the major influence of FiT in inverse relationship with PBP. A decrease in FiT causes the increase in the PBP and vice

TABLE 6. Different demand scenarios for sensitivity analysis.

% Change in load demand	LEC (Cents/kWh)	PBP (years)	Duration of generator operation (hour)
-20	6.39	6.56	7
-10	6.48	6.78	75
+10	7.03	9.63	548
+20	7.47	13.43	955

TABLE 7. Technical and economic specifications of HES components.

Component	Parameter	Variable	Values	Units
Solar PV	Rated power (per module)	P_{PV}	325	W
	Module efficiency	r	17.0	%
	Performance ratio	PR	0.75	-
	Initial (capital) cost [70]	IC_{PV}	305	$/kW
	Operating cost (yearly) [70]	OC_{PV}	3.05	$/kW
	Expected lifetime	$Life_{PV}$	25	Years
Wind turbine	Rated power	P_{WT}	5	kW
	Start-up wind speed	$v_{cut\ in}$	3	m/s
	Survival wind speed	$v_{cut\ off}$	50	m/s
	Rated wind speed	v_{rated}	10	m/s
	Rotor diameter	-	5.4	m
	Blades	-	3	-
	Initial (capital) cost [71]	IC_{WT}	600	$/kW
	Operating cost (yearly) [71]	OC_{WT}	6.0	$/kW
	Expected lifetime	$Life_{WT}$	25	Years
Lead acid batteries	Rated capacity	C_{Bat}	1800	Wh
	Charging/discharging efficiency	η_{Bat}	100	%
	Initial (capital) cost	IC_{Bat}	250	$/kWh
	Replacement cost (After 5 years)	RC_{Bat}	250	$/kWh
	Expected lifetime	$Life_{Bat}$	5	Years
Diesel generator	Rated power	P_{Gen}	10+20	kW
	Generator efficiency	η_{Gen}	85.0	%
	Power factor	PF	0.8	-
	Initial (capital) cost	IC_{Gen}	180	$/kW
	Operating cost (yearly) [71]	OC_{Gen}	0.064	$/Hour
	Fuel cost	FC_{Gen}	0.690	$/Liter
	CO_2 emissions [72]	CO_2	0.27	Kg/kWh
	Expected lifetime	$Life_{Gen}$	15000	Hours
Inverter	Rated power	P_{inv}	30	kW
	Inverter efficiency	η_{inv}	95	%
	Initial (capital) cost	IC_{Inv}	1669	$
	Replacement cost (After 10 years)	RC_{Inv}	1669	$
	Expected lifetime	$Life_{Inv}$	10	Years
Important project parameters	Project lifetime [54]	N	25	Years
	Discount rate [54]	r	9	%
	PV degradation rate [54]	DEG_{PV}	0.50	%
	WT degradation rate [73]	DEG_{WT}	0.60	%
	Fuel curve intercept coefficient [11]	C_1	0.246	L/kWh
	Fuel curve slope [11]	C_2	0.0814	L/kWh
	Feed in tariff	FiT	12	Cents/kWh
	Time-of-use tariff (Off-peak time)	$TOU_{Off\text{-}peak}$	9.3	Cents/kWh
	Time-of-use (Peak time)	TOU_{Peak}	13.1	Cents/kWh
Balance of system cost	[74]	BOS	1000	$

versa. This is because the revenue from HES is generated by selling all the generated electricity at the applicable FiT.

2) CLIMATOLOGICAL PARAMETERS

The uncertainties and intermittencies of the irradiance levels and wind speed are reflected by the changes in the PV power

(P_{PV}), and WT power (P_{WT}), respectively. For completeness, the changes in the battery capacity (P_{BSU}) are considered too. Similar to the previous exercise, the sensitivity analysis is carried out for $\pm$ 10% and $\pm$ 20% changes in the values of P_{PV}, P_{WT} and P_{BSU}. Similar to the previous exercise, the sensitivity analysis is carried out for $\pm$ 10% and $\pm$ 20% changes in the values of P_{PV}, P_{WT} and P_{BSU}. The results of these scenarios with respect to LEC and PBP are presented in Figure 17 It can be observed that PV and WT. power has an inverse correlation with the LEC; higher PV and WT power results in the lower LEC, and vice versa. It can be observed that PV and WT power has an inverse correlation with the LEC; higher PV and WT power results in the lower LEC, and vice versa. While for the BSU, the LEC increases with both increment and decrement in its capacity. The increase of LEC with battery capacity is expected—simply because of the higher capital cost of larger batteries.

On the other hand, the increase of LEC with decreased battery capacity is not straightforward. It can be explained in the context of the HES optimization, where reducing the installed capacity of BSU allows the diesel generators to compensate for the demand. This in turn, increases the LEC because of the high operational cost of diesel generators. The impact of the changes in the climatological parameters on the PBP is depicted in plot (b). Clearly the increase in the PV and BSU power decreases the PBP, and vice versa. The PV being the main renewable source of the HES has its higher impact while the WT has least impact due to its very low contribution for HES.

3) VARIATION IN LOAD DEMAND

Finally, the sensitivity analysis is conducted to determine the impact of varying the load demand to the LEC and the PBP. The objective is to assess the capability of HES with respect to the future changes in the load demand. The analysis is performed by varying the demand by $\pm$10% and $\pm$20%. The results are shown in Table 6. For the given configuration of HES, the LEC and PBP are directly proportional to load demand. If the demand increases, LEC and PBP increase, and vice versa. This is due to the increase in the generator working hours. Furthermore, the obtained configuration of the HES is still profitable for the load variations of $\pm$ 10% and $\pm$ 20% scenarios. For these figures, the notice PBP is still within the life span of the project (25 years). However, when the overall demand is increased to 37%, the PBP reaches 25.3 years that exceeds the life span limit. At this point, several actions can be considered to reduce the PBP of the system: 1) system expansion by incorporating more renewables or storage, and 2) revision of FiT, tax and subsidies mechanism. These results can help policy makers and analysts to design a reliable and cost-effective power system.

V. CONCLUSION

This study presented optimal design and performance analysis of hybrid energy system (HES) with the aim to ensure uninterrupted power supply during grid load shedding. The optimization process is inclusive, integrating local weather conditions, load demand, and community-specific load shedding schedules tailored to a small residential community in Balochistan, Pakistan. The HES's optimal configuration modelled using photovoltaic modules (35.5kW), wind turbines (10kW), and battery storage (28.8kW), yielded a levelized electricity cost (LEC) of 6.64 cents/kWh and a payback period (PBP) of 7.4 years. These results indicate HES potential to address load shedding problem as the computed LEC is cheaper than grid electricity price of 9.3cents/kWh. Furthermore, the breakeven point of 7.4 years proves to be an attractive proposition, especially considering the 25-year lifespan of the HES project. To evaluate its performance against load shedding, the HES is compared with conventional systems, including uninterruptible power supplies (UPS), standalone diesel generators, and a combined UPS-generator, all tested under identical operating conditions.

The findings reveal that the HES is 49.8%, 77.6%, and 66.7% more cost-efficient than the UPS, generator, and combined UPS-generator systems, respectively. These results demonstrate the significant superiority of the HES over conventional solutions. This study adopts a comprehensive approach, covering the optimal design of the HES, performance evaluation, and sensitivity analysis, aiming to present a holistic understanding of addressing the energy deficit challenges faced by many developing countries. The findings offer valuable insights for policymakers, investors, and stakeholders involved in sustainable energy solutions. These insights can guide informed decision-making and strategic initiatives, contributing to the development of a more resilient and efficient energy landscape. Future work could explore the feasibility of the HES for random and unscheduled power outages, expanding its applicability and potential impact.

APPENDIX

See in Table 7.

ACKNOWLEDGMENT

The authors extend their gratitude to Universiti Tun Hussein Onn Malaysia and Universiti Teknologi Malaysia for their invaluable support and contributions.

REFERENCES

[1] S. M. Hossain and M. M. Hasan, "Energy management through biogas based electricity generation system during load shedding in rural areas," *TELKOMNIKA, Telecommunication Comput. Electron. Control*, vol. 16, no. 2, pp. 525–532, Apr. 2018, doi: 10.12928/TELKOMNIKA.v16i2.5190.

[2] H. Bevrani, A. G. Tikdari, and T. Hiyama, "Power system load shedding: Key issues and new perspectives," *World Acad. Sci. Eng. Technol.*, vol. 65, pp. 199–204, 2010.

[3] P. Lakra and M. Kirar, "Load sheddingtechniques for system with cogeneration: A review," *Electr. Electron. Eng., Int. J.*, vol. 4, no. 3, pp. 83–96, Aug. 2015, doi: 10.14810/elelij.2015.4307.

[4] T. Adefarati and R. C. Bansal, "Reliability, economic and environmental analysis of a microgrid system in the presence of renewable energy resources," *Appl. Energy*, vol. 236, pp. 1089–1114, Feb. 2019, doi: 10.1016/j.apenergy.2018.12.050.

[5] S. Rehman, N. Natrajan, M. Mohandes, L. M. Alhems, Y. Himri, and A. Allouhi, "Feasibility study of hybrid power systems for remote dwellings in Tamil Nadu, India," *IEEE Access*, vol. 8, pp. 143881–143890, 2020.

[6] M. P. Bakht, Z. Salam, A. R. Bhatti, W. Anjum, S. A. Khalid, and N. Khan, "Stateflow-based energy management strategy for hybrid energy system to mitigate load shedding," *Appl. Sci.*, vol. 11, no. 10, p. 4601, May 2021.

[7] K. Anoune, A. Laknizi, M. Bouya, A. Astito, and A. B. Abdellah, "Sizing a PV-wind based hybrid system using deterministic approach," *Energy Convers. Manage.*, vol. 169, pp. 137–148, Aug. 2018.

[8] M. P. Bakht, Z. Salam, A. R. Bhatti, U. U. Sheikh, N. Khan, and W. Anjum, "Techno-economic modelling of hybrid energy system to overcome the load shedding problem: A case study of Pakistan," *PLoS ONE*, vol. 17, no. 4, Apr. 2022, Art. no. e0266660, doi: 10.1371/journal.pone.0266660.

[9] A. L. Bukar, C. W. Tan, L. K. Yiew, R. Ayop, and W.-S. Tan, "A rule-based energy management scheme for long-term optimal capacity planning of grid-independent microgrid optimized by multi-objective grasshopper optimization algorithm," *Energy Convers. Manage.*, vol. 221, Oct. 2020, Art. no. 113161, doi: 10.1016/j.enconman.2020.113161.

[10] Z. A. Vale, C. Ramos, P. Faria, J. P. Soares, B. Canizes, J. Teixeira, and H. M. Khodr, "Comparison between deterministic and meta-heuristic methods applied to ancillary services dispatch," in *Proc. Int. Conf. Ind., Eng. Other Appl. Appl. Intell. Syst.*, 2010, pp. 731–741.

[11] A. L. Bukar, C. W. Tan, and K. Y. Lau, "Optimal sizing of an autonomous photovoltaic/wind/battery/diesel generator microgrid using grasshopper optimization algorithm," *Sol. Energy*, vol. 188, pp. 685–696, Aug. 2019, doi: 10.1016/j.solener.2019.06.050.

[12] U. Sultana, A. B. Khairuddin, B. Sultana, N. Rasheed, S. H. Qazi, and N. R. Malik, "Placement and sizing of multiple distributed generation and battery swapping stations using grasshopper optimizer algorithm," *Energy*, vol. 165, pp. 408–421, Dec. 2018, doi: 10.1016/j.energy.2018.09.083.

[13] M. D. A. Al-falahi, S. D. G. Jayasinghe, and H. Enshaei, "A review on recent size optimization methodologies for standalone solar and wind hybrid renewable energy system," *Energy Convers. Manage.*, vol. 143, pp. 252–274, Jul. 2017.

[14] T. Bambaravanage, S. Kumarawadu, and A. Rodrigo, "Comparison of three under-frequency load shedding schemes referring to the power system of Sri Lanka," *Engineer: J. Inst. Engineers, Sri Lanka*, vol. 49, no. 1, p. 41, Jan. 2016.

[15] J. A. Laghari, H. Mokhlis, A. H. A. Bakar, and H. Mohamad, "Application of computational intelligence techniques for load shedding in power systems: A review," *Energy Convers. Manage.*, vol. 75, pp. 130–140, Nov. 2013, doi: 10.1016/j.enconman.2013.06.010.

[16] J. A. P. Lopes, C. L. Moreira, A. G. Madureira, F. O. Resende, X. Wu, N. Jayawarna, Y. Zhang, N. Jenkins, F. Kanellos, and N. Hatziargyriou, "Control strategies for microgrids emergency operation," in *Proc. Int. Conf. Future Power Syst.*, 2005, p. 6.

[17] P. Warren, "A review of demand-side management policy in the U.K.," *Renew. Sustain. Energy Rev.*, vol. 29, pp. 941–951, Jan. 2014.

[18] L. Gelazanskas and K. A. A. Gamage, "Demand side management in smart grid: A review and proposals for future direction," *Sustain. Cities Soc.*, vol. 11, pp. 22–30, Feb. 2014.

[19] H. Syadli, M. P. Abdullah, M. Y. Hassan, and F. Hussin, "Demand side management for reducing rolling blackouts due to power supply deficit in Sumatra," *J. Teknol., Sci. Eng.*, vol. 69, no. 5, pp. 39–43, 2014, doi: 10.11113/jt.v69.3202.

[20] B. Liu, J. R. Lund, S. Liao, X. Jin, L. Liu, and C. Cheng, "Peak shaving model for coordinated hydro-wind-solar system serving local and multiple receiving power grids via HVDC transmission lines," *IEEE Access*, vol. 8, pp. 60689–60703, 2020.

[21] N. U. Blum, R. Sryantoro Wakeling, and T. S. Schmidt, "Rural electrification through village grids—Assessing the cost competitiveness of isolated renewable energy technologies in Indonesia," *Renew. Sustain. Energy Rev.*, vol. 22, pp. 482–496, Jun. 2013, doi: 10.1016/j.rser.2013.01.049.

[22] J. Khoury, R. Mbayed, G. Salloum, and E. Monmasson, "Optimal sizing of a residential PV-battery backup for an intermittent primary energy source under realistic constraints," *Energy Buildings*, vol. 105, pp. 206–216, Oct. 2015, doi: 10.1016/j.enbuild.2015.07.045.

[23] M. Zubair, A. B. Awan, M. M. Rehman, M. N. Khan, and G. Abbas, "Residential and commercial UPS user's contribution to load shedding and possible solutions using renewable energy," *Energy Policy*, vol. 151, Mar. 2020, Art. no. 112194, doi: 10.1016/j.enpol.2021.112194.

[24] N. Arshad and U. Ali, "An analysis of the effects of residential uninterpretable power supply systems on Pakistan's power sector," *Energy Sustain. Develop.*, vol. 36, pp. 16–21, Feb. 2017, doi: 10.1016/j.esd.2016.09.004.

[25] M. B. Najjar, A. Alameddine, and P. G. Horkos, "Supervisory control for sectored distributed generation during load shedding in lebanon's power grid," in *Proc. IEEE Int. Conf. Renew. Energy Res. Appl. (ICRERA)*, Nov. 2016, pp. 73–78.

[26] A. Hooshmand, B. Asghari, and R. Sharma, "A power management system for planned & unplanned grid electricity outages," in *Proc. IEEE PES Innov. Smart Grid Technol. Latin Amer. (ISGT LATAM)*, Oct. 2015, pp. 382–386.

[27] P. M. Murphy, S. Twaha, and I. S. Murphy, "Analysis of the cost of reliable electricity: A new method for analyzing grid connected solar, diesel and hybrid distributed electricity systems considering an unreliable electric grid, with examples in Uganda," *Energy*, vol. 66, pp. 523–534, Mar. 2014.

[28] K. Siraj, M. Awais, H. A. Khan, A. Zafar, A. Hussain, N. A. Zaffar, and S. H. I. Jaffery, "Optimal power dispatch in solar-assisted uninterruptible power supply systems," *Int. Trans. Electr. Energy Syst.*, vol. 30, no. 1, pp. 1–15, Jan. 2020, doi: 10.1002/2050-7038.12157.

[29] V. A. Ani, "Design of a reliable hybrid (PV/diesel) power system with energy storage in batteries for remote residential home," *J. Energy*, vol. 2016, pp. 1–16, Aug. 2016, doi: 10.1155/2016/6278138.

[30] S. M. Amrr, M. S. Alam, M. S. J. Asghar, and F. Ahmad, "Low cost residential microgrid system based home to grid (H2G) back up power management," *Sustain. Cities Soc.*, vol. 36, pp. 204–214, Jan. 2018.

[31] L. M. Halabi and S. Mekhilef, "Flexible hybrid renewable energy system design for a typical remote village located in tropical climate," *J. Cleaner Prod.*, vol. 177, pp. 908–924, Mar. 2018, doi: 10.1016/j.jclepro.2017.12.248.

[32] L. Tripathi, A. K. Mishra, A. K. Dubey, C. B. Tripathi, and P. Baredar, "Renewable energy: An overview on its contribution in current energy scenario of India," *Renew. Sustain. Energy Rev.*, vol. 60, pp. 226–233, Jul. 2016.

[33] A. Bhattacharjee, H. Samanta, A. Ghosh, T. K. Mallick, S. Sengupta, and H. Saha, "Optimized integration of hybrid renewable sources with long-life battery energy storage in microgrids for peak power shaving and demand side management under different tariff scenario," *Energy Technol.*, vol. 9, no. 9, Sep. 2021, Art. no. 2100199.

[34] D. Kumar Lal, B. Bhusan Dash, and A. K. Akella, "Optimization of PV/wind/micro-hydro/diesel hybrid power system in Homer for the study area," *Int. J. Electr. Eng. Informat.*, vol. 3, no. 3, pp. 307–325, Sep. 2011.

[35] E. Jamil, S. Hameed, B. Jamil, and Qurratulain, "Power quality improvement of distribution system with photovoltaic and permanent magnet synchronous generator based renewable energy farm using static synchronous compensator," *Sustain. Energy Technol. Assessments*, vol. 35, pp. 98–116, Oct. 2019.

[36] M. Z. Malik, A. Ali, G. S. Kaloi, A. M. Soomro, M. H. Baloch, and S. T. Chauhdary, "Integration of renewable energy project: A technical proposal for rural electrification to local communities," *IEEE Access*, vol. 8, pp. 91448–91467, 2020, doi: 10.1109/ACCESS.2020.2993903.

[37] M. S. Ismail, M. Moghavvemi, T. M. I. Mahlia, K. M. Muttaqi, and S. Moghavvemi, "Effective utilization of excess energy in standalone hybrid renewable energy systems for improving comfort ability and reducing cost of energy: A review and analysis," *Renew. Sustain. Energy Rev.*, vol. 42, pp. 726–734, Feb. 2015.

[38] J. Rocabert, A. Luna, F. Blaabjerg, and P. Rodríguez, "Control of power converters in AC microgrids," *IEEE Trans. Power Electron.*, vol. 27, no. 11, pp. 4734–4749, Nov. 2012.

[39] J. Martin, "Distributed vs. centralized electricity generation: Are we witnessing a change of paradigm?" *Introduction Distrib. Gener.*, May 2009.

[40] K. R. Khalilpour and A. Vassallo, "Technoeconomic parametric analysis of PV-battery systems," *Renew. Energy*, vol. 97, pp. 757–768, Nov. 2016, doi: 10.1016/j.renene.2016.06.010.

[41] H. Rezk, M. Al-Dhaifallah, Y. B. Hassan, and H. A. Ziedan, "Optimization and energy management of hybrid photovoltaic-diesel-battery system to pump and desalinate water at isolated regions," *IEEE Access*, vol. 8, pp. 102512–102529, 2020.

[42] X. Xu, W. Hu, D. Cao, Q. Huang, C. Chen, and Z. Chen, "Optimized sizing of a standalone PV-wind-hydropower station with pumped-storage installation hybrid energy system," *Renew. Energy*, vol. 147, pp. 1418–1431, Mar. 2020, doi: 10.1016/j.renene.2019.09.099.

[43] A. Ilinca, E. McCarthy, J. L. Chaumel, and J. L. Rétiveau, "Wind potential assessment of Quebec Province," *Renew. Energy*, vol. 28, no. 12, pp. 1881–1897, 2003, doi: 10.1016/S0960-1481(03)00072-7.

[44] S. Mohseni and A. C. Brent, "Economic viability assessment of sustainable hydrogen production, storage, and utilisation technologies integrated into on- and off-grid micro-grids: A performance comparison of different meta-heuristics," *Int. J. Hydrogen Energy*, vol. 45, no. 59, pp. 34412–34436, Dec. 2020, doi: 10.1016/j.ijhydene.2019.11.079.

[45] S. Jeon, J.-J. Yun, and S. Bae, "Comparative study on the battery state-of-charge estimation method," *Indian J. Sci. Technol.*, vol. 8, no. 26, pp. 1–6, Oct. 2015, doi: 10.17485/ijst/2015/v8i26/81677.

[46] A. S. O. Ogunjuyigbe, T. R. Ayodele, and O. A. Akinola, "Optimal allocation and sizing of PV/wind/split-diesel/battery hybrid energy system for minimizing life cycle cost, carbon emission and dump energy of remote residential building," *Appl. Energy*, vol. 171, pp. 153–171, Jun. 2016, doi: 10.1016/j.apenergy.2016.03.051.

[47] R. Belfkira, L. Zhang, and G. Barakat, "Optimal sizing study of hybrid wind/PV/diesel power generation unit," *Sol. Energy*, vol. 85, no. 1, pp. 100–110, Jan. 2011, doi: 10.1016/j.solener.2010.10.018.

[48] L. Zhang, G. Barakat, and A. Yassine, "Design and optimal sizing of hybrid PV/wind/diesel system with battery storage by using DIRECT search algorithm," in *Proc. 15th Int. Power Electron. Motion Control Conf. (EPE/PEMC)*, Sep. 2012, pp. 1–7, doi: 10.1109/EPEPEMC.2012.6397335.

[49] E. I. Vrettos and S. A. Papathanassiou, "Operating policy and optimal sizing of a high penetration RES-BESS system for small isolated grids," *IEEE Trans. Energy Convers.*, vol. 26, no. 3, pp. 744–756, Sep. 2011, doi: 10.1109/TEC.2011.2129571.

[50] A. Maleki, M. Ameri, and F. Keynia, "Scrutiny of multifarious particle swarm optimization for finding the optimal size of a PV/wind/battery hybrid system," *Renew. Energy*, vol. 80, pp. 552–563, Aug. 2015, doi: 10.1016/j.renene.2015.02.045.

[51] *Load Management Portal*, Ministry Energy (Power Division), Islamabad, Pakistan, 2020.

[52] M. P. Bakht, Z. Salam, and A. R. Bhatti, "Investigation and modelling of load shedding and its mitigation using hybrid renewable energy system," in *Proc. IEEE 7th Int. Conf. Power Energy (PECon)*, Dec. 2018, pp. 35–40, doi: 10.1109/PECON.2018.8684040.

[53] J. Aldersey-Williams and T. Rubert, "Levelised cost of energy—A theoretical justification and critical assessment," *Energy Policy*, vol. 124, pp. 169–179, Jan. 2019, doi: 10.1016/j.enpol.2018.10.004.

[54] Y. Khawaja, A. Allahham, D. Giaouris, C. Patsios, S. Walker, and I. Qiqieh, "An integrated framework for sizing and energy management of hybrid energy systems using finite automata," *Appl. Energy*, vol. 250, pp. 257–272, Sep. 2019.

[55] A. W. Dowling, T. Zheng, and V. M. Zavala, "Economic assessment of concentrated solar power technologies: A review," *Renew. Sustain. Energy Rev.*, vol. 72, pp. 1019–1032, May 2017, doi: 10.1016/j.rser.2017.01.006.

[56] Y. Zhang, T. Ma, P. E. Campana, Y. Yamaguchi, and Y. Dai, "A techno-economic sizing method for grid-connected household photovoltaic battery systems," *Appl. Energy*, vol. 269, Jul. 2020, Art. no. 115106, doi: 10.1016/j.apenergy.2020.115106.

[57] T. Ma and M. S. Javed, "Integrated sizing of hybrid PV-wind-battery system for remote island considering the saturation of each renewable energy resource," *Energy Convers. Manage.*, vol. 182, pp. 178–190, Feb. 2019, doi: 10.1016/j.enconman.2018.12.059.

[58] A. Maleki and A. Askarzadeh, "Artificial bee swarm optimization for optimum sizing of a stand-alone PV/WT/FC hybrid system considering LPSP concept," *Sol. Energy*, vol. 107, pp. 227–235, Sep. 2014, doi: 10.1016/j.solener.2014.05.016.

[59] O. Grodzevich and O. Romanko, "Normalization and other topics in multi-objective optimization," in *Proc. Fields-MITACS Ind. Problems Workshop*, vol. 2, Aug. 2006, pp. 89–101.

[60] X. Li, D. Hui, and X. Lai, "Battery energy storage station (BESS)-based smoothing control of photovoltaic (PV) and wind power generation fluctuations," *IEEE Trans. Sustain. Energy*, vol. 4, no. 2, pp. 464–473, Apr. 2013, doi: 10.1109/TSTE.2013.2247428.

[61] Y. Meraihi, A. B. Gabis, S. Mirjalili, and A. Ramdane-Cherif, "Grasshopper optimization algorithm: Theory, variants, and applications," *IEEE Access*, vol. 9, pp. 50001–50024, 2021, doi: 10.1109/ACCESS.2021.3067597.

[62] N. Engerer. (2020). Historical and Typical Meteorological Year. Solcast, Sydney, NSW, Australia. Accessed: Aug. 8, 2020. [Online]. Available: https://solcast.com/historical-and-tmy/

[63] S. A. Mirjalili, "Grasshopper optimization algorithm," *Adv. Eng. Softw.*, 2017. Accessed: Sep. 1, 2020. [Online]. Available: https://seyedalimirjalili.com/projects

[64] A. AlKassem, A. Draou, A. Alamri, and H. Alharbi, "Design analysis of an optimal microgrid system for the integration of renewable energy sources at a university campus," *Sustainability*, vol. 14, no. 7, p. 4175, Mar. 2022.

[65] B. Akarsu and M. S. Genç, "Optimization of electricity and hydrogen production with hybrid renewable energy systems," *Fuel*, vol. 324, Sep. 2022, Art. no. 124465.

[66] M. T. Castro, J. D. A. Pascasio, L. L. Delina, P. H. M. Balite, and J. D. Ocon, "Techno-economic and financial analyses of hybrid renewable energy system microgrids in 634 Philippine off-grid islands: Policy implications on public subsidies and private investments," *Energy*, vol. 257, Oct. 2022, Art. no. 124599, doi: 10.1016/j.energy.2022.124599.

[67] R. Chaurasia, S. Gairola, and Y. Pal, "Technical, economic, and environmental performance comparison analysis of a hybrid renewable energy system based on power dispatch strategies," *Sustain. Energy Technol. Assessments*, vol. 53, Oct. 2022, Art. no. 102787.

[68] M. M. M. Islam, A. Kowsar, A. K. M. M. Haque, M. K. Hossain, M. H. Ali, M. H. K. Rubel, and M. F. Rahman, "Techno-economic analysis of hybrid renewable energy system for healthcare centre in northwest Bangladesh," *Process Integr. Optim. Sustainability*, vol. 7, nos. 1–2, pp. 315–328, Mar. 2023.

[69] S. Vakili, A. Schönborn, and A. I. Ölçer, "Techno-economic feasibility of photovoltaic, wind and hybrid electrification systems for stand-alone and grid-connected shipyard electrification in Italy," *J. Cleaner Prod.*, vol. 366, Sep. 2022, Art. no. 132945.

[70] *Ultimate Solution for All Electronics and IT Needs*, W11stop Solar UPS Stabilizer, Karachi, Pakistan, 2021.

[71] *E-Commerce Company*, Alibaba Group, Hangzhou, China, 2021.

[72] V. Quaschning. (2020). *Specific Carbon Dioxide Emissions of Various Fuels*. Accessed: Sep. 1, 2020. [Online]. Available: https://www.volker-quaschning.de/datserv/CO2-spez/index_e.php

[73] I. Staffell and R. Green, "How does wind farm performance decline with age?" *Renew. Energy*, vol. 66, pp. 775–786, Jun. 2014, doi: 10.1016/j.renene.2013.10.041.

[74] D. Feldman, V. Ramasamy, R. Fu, A. Ramdas, J. Desai, and R. Margolis, "US solar photovoltaic system and energy storage cost benchmark: Q1 2020," Nat. Renew. Energy Lab. (NREL), Golden, CO, USA, Tech. Rep. NREL/TP-6A20-77324, Jan. 2021.

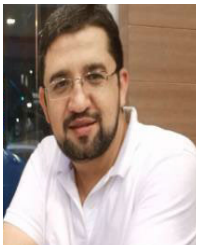

MUHAMMAD PAEND BAKHT received the Ph.D. degree in electrical engineering from the University of Technology Malaysia. He is a Postdoctoral Researcher with Universiti Tun Hussein Onn Malaysia. Before the doctoral journey, he was an Assistant Professor with the Faculty of Information and Communication Technology, Balochistan University of Information Technology, Engineering and Management Sciences (BUITEMS), Quetta, Pakistan. Currently, he is on study leave from BUITEMS to pursue his passion for further research. He has authored several research articles in reputable journals and presented his research ideas at international conferences. His research interests include optimization and energy management of grid connected renewable energy systems. His current research extends toward smart grid technologies and the innovative application of machine learning for predictive forecasting.

MOHD NORZALI HAJI MOHD (Senior Member, IEEE) received the B.Eng. and M.Eng. degrees from Fukui University, Japan, in 2002 and 2004, respectively, and the Ph.D. degree from the Department of Information Sciences and Biomedical Engineering, Kagoshima University, Japan, April 2015. He is an Associate Professor with the Department of Computer Engineering, Faculty of Electrical and Electronic Engineering, Universiti Tun Hussein Onn Malaysia (UTHM). Previously, he was a Faculty Laboratory Manager (HoD) and an Industrial Training Coordinator with UTHM.

USMAN ULLAH SHEIKH received the B.Eng. degree in electrical and mechatronics engineering, the M.Eng. degree in telecommunications engineering, and the Ph.D. degree in image processing and computer vision from Universiti Teknologi Malaysia (UTM), in 2003, 2005, and 2009, respectively. He is currently a Senior Lecturer with the School of Electrical Engineering, UTM, where he is also an Office Bearer of Academic Manager with the School of Electrical Engineering. He has published more than 100 research papers in well reputed journals and conferences. His research interests include computer vision, machine learning, and embedded systems design.

NUZHAT KHAN received the M.S. degree in information technology from the Balochistan University of Information Technology, Engineering and Management Science (BUITEMS), Quetta, Pakistan, in 2019, and the Ph.D. degree in environmental technology from the School of Industrial Technology, University of Science Malaysia. Currently she is part of the research group at VeCAD (VLSI and Embedded Computing Architecture Design) laboratory, University of Technology Malaysia. She received the Higher Education Commission (HEC) Scholarship for the master's study. Her research interests include image processing, natural language processing, applied linguistics, statistical linguistics, artificial intelligence, machine learning, and deep learning.